REPORT

SP 4 FoU Snøskred

ANNUAL REPORT 2017

DOC.NO. 20170131-05-R
REV.NO. 0 / 2018-01-12

NORWEGIAN GEOTECHNICAL INSTITUTE
NGI.NO

Project

Project title:	SP 4 FoU Snøskred
Document title:	Annual Report 2017
Document no.:	20170131-05-R
Date:	2018-01-12
Revision no. /rev. date:	0 /

Client

Client:	Norges vassdrags- og energidirektorat (NVE)
Client contact person:	Aart Verhage and Odd Are Jensen
Contract reference:	Tildelingsbrev fra NVE til NGI, 2017-11-30

for NGI

Project manager:	Dieter Issler
Prepared by:	Dieter Issler, Peter Gauer, Kjersti Gisnås, Sylfest Glimsdal, Christian Jaedicke and Frode Sandersen
Reviewed by:	Ulrik Domaas

NORWEGIAN GEOTECHNICAL INSTITUTE
NGI.NO

Main office
PO Box 3930 Ullevaal St.
NO-0806 Oslo
Norway

Trondheim office
PO Box 5687 Torgarden
NO-7485 Trondheim
Norway

T 22 02 30 00
F 22 23 04 48
NGI@ngi.no

BIC NO. DNBANOKK
IBAN NO26 5096 05 01281
ORGANISATION NO.
958 254 318MVA

ISO 9001/14001
CERTIFIED BY BSI
FS 32989/EMS 612006

Summary

During the first year of the project period 2017–2019 of NGI's research project on snow avalanches, work was carried out in all five work packages (WP 1 – Ryggfonn and model development, WP 2 – Statistical tools, WP 3 – Slushflows, WP 4 – Investigation of relevant avalanche events, WP 5 – Improved tools for local avalanche forecasting). The results of the research have been presented at national and international conferences and published in renowned peer-reviewed journals as well as in conference proceedings and reports.

In WP 1, the winter was once more disappointing with regard to avalanche experiments at Ryggfonn, but continued analysis of Ryggfonn data from previous years and published measurements around the globe confirmed the validity of a scaling relation for the maximum avalanche velocity in terms of the drop height. This implies that the effective friction along the avalanche path varies much less than predicted by usually applied calibration of Voellmy-type models. An in-depth analysis of extensions to the Voellmy model of avalanche movement that were proposed by SLF was published and attracted considerable interest.

StatPack, a tool for predicting avalanche impact probability at the local level based on statistical tools, reached the stage where first tests could be conducted. They confirmed the viability of the approach and showed which modules need to be improved in 2018. This work proved to be much more time-consuming than anticipated and required significant reallocation of resources from WPs 3 and 5 to WP 2.

Activity in WP 3 was therefore focused on further tests with snowcover simulations that will be useful not only for slushflow prediction, but in avalanche forecasting in general. The Circum-Arctic Slushflow Network coordinate by NGI is gradually picking up momentum.

Three very different avalanche events were investigated in 2017 within WP 4: a relatively small avalanche that destroyed two houses in Longyearbyen next to the location of the 2015 disaster; a small and strongly fluidized avalanche on the Hardangervidda that caught six ski tourists who miraculously survived, and the devastating avalanche at Rigopiano in the Apennines of central Italy. Analysis of the collected data from Rigopiano is still ongoing. The same is the case for the data from a joint project on avalanche detection by infrasound carried out in Grasdalen.

Competence in simulating wind fields in alpine terrain (using the code WindSim) has been built up in WP 5. Pre-calculated local windfields for different synoptic situations will be a useful supporting tool for local avalanche forecasting and hazard mapping. WP 5 furthermore developed tools for extracting and analyzing gridded nivo-meteorological or climatological data from SeNorge that are of great value for avalanche hazard mapping.

Contents

Review and reference page

1 Overview and administrative aspects

1.1 Project goals in 2017

Table 1 Summary of project goals 2017, based on the project proposal

WP 1	Maintenance of full-scale test site Ryggfonn and research station Fonnbu Full-scale experiments at Ryggfonn with artificial release Contribution to development of dynamical models
WP 2	Finish implementation of the statistical framework for local forecasting Tests of the statistical framework, possibly adjustments Integration of StatPack into NGI's processes for local avalanche forecasting
WP 3	Snowcover simulations with SNOWPACK Attempt at simulating slushflows by tuning parameters of avalanche models
WP 4	Site investigations and analyses of interesting avalanche events Detection of avalanches by means of infrasound
WP 5	Install and get familiar with WindSim Study wind field patterns mountain terrain through simulations

1.2 Use of human and financial resources

The contributors to the project in 2017 are listed alphabetically in Table 2, together with the work package(s) and main topic(s) of their work. Table 3 gives an overview of the planned and actual allocation of resources to the different work packages (including WP 0 – Project administration).

In the course of the reporting period, it became clear that completing and testing the statistical framework for local avalanche forecasting, StatPack, and then introducing it into the daily work routines of the avalanche forecasting group required a substantially larger effort than anticipated in the autumn of 2016, when the project plan was developed. This was compensated by reduced activity and expenditures in WPs 3 and 5.

1.3 Summary of results

The results obtained in each work package are presented in more detail in the following chapters and, in some cases, in dedicated reports. For the readers' convenience, an "executive summary" is given here.

Once again, the winter was disappointing with regard to the possibility for full-scale experiments at Ryggfonn; the campaign in the second half of March resulted only in a small avalanche that stopped shortly below the release area. On the other hand, there were three spontaneous avalanche events that were investigated: With 29 deaths, the Rigopiano avalanche (central Italy) was the third-most deadly snow avalanche in Europe

since World War II. Of particular interest was also the very extensive damage to the forest (Issler, 2018). Only about a year after the deadly avalanche of 2015, another avalanche destroyed two houses in Longyearbyen, but fortunately did not claim lives. The third near Haugastøl (Hardangervidda) was remarkable due to its extent, triggering and the fact that a completely buried person survived without a breathing space, yet conscious and essentially non-injured, for four hours (Brattlien, 2017).

Table 2 Contributors to the project in 2017, listed alphabetically

Name	WP	Topic
Kjetil Brattlien	4	Investigation of avalanche events
Ulrik Domaas	SG 1	Member of Steering Group, QA Follow-up on instrumented deflection dam at Gudvangen
Peter Gauer	1 3 5	WP leader, Ryggfonn experiments, data analysis Analysis of video of slushflow event WindSim
Kjersti Gisnås	1 3 5	Ryggfonn experiment Co-advisor for MSc thesis of S. Jordet WP leader, WindSim, analysis of SeNorge.no climate data
Sylfest Glimsdal	2 5	WP leader, program implementation WindSim
Dieter Issler	PL 1 2 4	Project leadership and administration, QA Model development QA run-out modeling Investigation of avalanche event
Christian Jaedicke	2 3	QA release probability WP leader, Circum-Arctic Slushflow Network
Árni Jónsson	4	Investigation of avalanche event
Sigurd Jordet	3	Snow-cover simulation (MSc thesis at Univ. of Oslo)
Krister Kristensen	1 4	Ryggfonn maintenance and experiment Avalanche detection by infrasound
Erik Lied	1	Maintenance of the Ryggfonn measurement system
Galina Ragulina	PA	Project Assistant (on maternal leave April–December)
Frode Sandersen	4	WP leader, QA
Helge Smebye	1	Ryggfonn – experiment and LiDaR data analysis
Anders Solheim	SG 3	Member of Steering Group Advisor for MSc thesis of S. Jordet
Marco Uzielli	2	Statistical methods for climate, avalanche release and run-out

Table 3 Budgeted and actual allocation of resources per work package in 2017 (all amounts in kNOK)

	WP 0	WP 1	WP 2	WP 3	WP 4	WP 5	Sum
Budget 2017	300	1100	350	350	600	300	3000
Used 2017	334	1215	599	172	577	104	3001
Difference	+34	+115	+249	–178	–23	–196	+1

Further work in WP 1 (Gauer, 2017, submitted; McClung and Gauer, submitted) continued the analysis of experimental data initiated earlier and completed a report, begun in the preceding project period 2014–2016, on the conjectured fluidizing effect of air pressed out of the snow cover by an avalanche flowing over it (Issler, 2017a). Moreover, an in-depth analysis of extensions to the Voellmy-type avalanche flow model RAMMS proposed by a group at WSL/SLF in Switzerland revealed a number of inconsistencies in their physical and mathematical formulations. The recently published paper has attracted considerable interest (Issler et al., 2017). In consulting work, SL-1D, a quasi-2D two-layer model for powder-snow avalanches (Issler, 1998) is occasionally used to estimate the pressure due to the cloud of suspended particles and the fully fluidized layer of intermediate density underneath it. In order to compensate approximately for some of the shortcomings of the model and to deal with the effect of protection dams, extensions were developed, but never documented in publicly accessible documents. To remedy this, an NGI Technical Note summarizing the model and detailing the extensions was written (Issler, 2017b).

Work on the statistical framework for quantifying avalanche danger in local avalanche forecasting (WP 2) has progressed substantially. Solutions to some of the conceptual problems of the run-out calculations that were identified at the end of the previous project period have been proposed recently. They need to be implemented and tested in 2018 together with some adjustments and fine-tuning in the module for release probability.

With WP 2 requiring more resources than planned, WPs 3 and 5 were less active. Nevertheless, valuable insight into the conditions for successful snow-cover modeling in Norway resulted from a MSc thesis at the University of Oslo, guided with financial support from the project (Jordet, 2017). Comparison of the numerical simulations with manual observations at the location of two automatic nivo-meteo stations was crucial in this work. Similarly, the limited work in WP 5 on extracting relevant information on local snow climate from the KliNoGrid data set (at 1 km^2 grid resolution) has been found to be of great value for hazard mapping.

1.4 Dissemination

Presentations at conferences, symposia and meetings

Domaas, U. and K. Gisnås. Avalanches in the context of climate change in the northern regions. Invited presentation at the International Symposium ‘Visions of avalanche protection’, Galtür, Austria, May 27–28, 2017.

Jaedicke, C., D. Issler and P. Gauer. “Her har det aldri gått skred før” – Hvor sjeldne og ekstreme er sjeldne og ekstreme skred? Oral presentation at Norsk snøskredkonferanse, Åndalsnes, Norway, November 10, 2017.

Gauer, P. Risk management technology in avalanche-prone areas. Invited presentation at the International Symposium ‘Visions of avalanche protection’, Galtür, Austria, May 27–28, 2017.

Jónsson, Á. Avalanches in Longyearbyen Svalbard 2015 and 2017. Invited presentation at the International Symposium 'Visions of avalanche protection', Galtür, Austria, May 27–28, 2017.

Publications

Domaas, U. and K. Gisnås (2017). Avalanches in the context of climate change in the northern regions. *Wildbach und Lawinenverbau* **81**(179), 70–79

Gauer, P. (2017). Risikomangement in lawinenexponierten Gebieten Norwegens. *Wildbach und Lawinenverbau* **81**(179), 100–111 (in German with English summary)

Gauer, P. (submitted). Considerations on scaling behavior in avalanche flow along cycloidal and parabolic tracks. *Cold Regions Science and Technology*

Issler, D., J. T. Jenkins and J. N. McElwaine (2017). Comments on avalanche flow models based on the concept of random kinetic energy. *Journal of Glaciology*, DOI 10.1017/jog.2017.62

Jónsson, Á. and C. Jaedicke (2017). Avalanches in Longyearbyen, Svalbard, 2015 and 2017. *Wildbach und Lawinenverbau* **81**(179), 182–187

McClung, D. M. and P. Gauer (submitted). Maximum frontal speeds, alpha angles and deposit volumes of flowing snow avalanches. *Cold Regions Science and Technology*.

Reports

Brattlien, K. (2017). Snøskredulykke ved Haugastøl 2017-03-15. NGI Technical Note 20170131-03-TN. Norwegian Geotechnical Institute, Oslo, Norway, 16 pages (in Norwegian)

Issler, D. (2017b). Snøskyskredmodell SL-1D – Grunnleggende ligninger og korrekturfaktorer. NGI Technical Note 20170131-06-TN. Norwegian Geotechnical Institute, Oslo, Norway, 10 pages (in Norwegian)

Issler, D. (2018). Field Survey of the 2017-01-18 Rigopiano avalanche. NGI Technical Note 20170131-02-TN. Norwegian Geotechnical Institute, Oslo, Norway

Web site

In the course of 2017, the web site from the preceding project period 2014–2016 (https://www.ngi.no/eng/Projects/Avalanche-research) was updated and all project documents of potential interest made publicly accessible to the extent allowed by copyright. Also, all presentations at the Topical Meeting on Snow Avalanches at Gardermoen Airport in November 2016 were made accessible through that web site.

The content of the pages for the present project period has been outlined, but needs to be developed into complete web pages in 2018. However, a separate web page for the Circum-Arctic Slushflow Network (CASN) has been set up (visit the page at https://www.ngi.no/Prosjekter/Circum-Arctic-Slushflow-Network-CASN or see Sec. 4.3 for further details).

2 WP 1 – Full-scale experiments at Ryggfonn and model development

2.1 Maintenance of the full-scale avalanche test site Ryggfonn

Under this task, necessary repairs and updating of the data acquisition system at the Ryggfonn avalanche test site were carried out so that the site is ready for the winter season 2017/2018. Lightning during summer damaged the data acquisition system. There occurred also some problems with the RADAR system during the avalanche tests. The RADAR system is now 15 years old and more technical problems will presumably arise in the future.

2.2 Experimental results from the full-scale test site Ryggfonn

2.2.1 Avalanche releases

Five spontaneous avalanches of size 2 to 3 (on the EAWS avalanche size scale) occurred during the winter 2016/2017. Figure 1 shows an example of data recorded during the event on 2017-01-03. Otherwise, no weather situation occurred that held promise for artificially releasing a sizeable avalanche and obtaining good-quality measurements. At the end of March, an artificial release was nevertheless attempted, but it resulted only in a small avalanche (EAWS size 2) that stopped in the upper track.

2.2.2 Analysis of LiDAR data from Ryggfonn, March 2017 and follow-up LiDAR tests

As part of the measurement protocol during the March campaign at Ryggfonn, the avalanche path was scanned with a laser scanner before and after the avalanche release attempt. NGIs long-range Optec Ilris LR LiDAR scanner was used for the purpose. The scanner was installed on the concrete pillar at Sætreskarsfjellet. As Figure 3 shows, the weather appeared sunny with good visibility during the campaign, even though it had been snowing earlier the same day.

The first scan was finished at approximately 13:30. Inspection of the collected data revealed that no usable data was collected. No laser beams seemed to reach the avalanche path. All laser pulses seemed to be returned by particles in a range of 0–300 m from the scanner. The same happened with the second scan taken after the attempt of releasing an avalanche. The results of the scan campaign are illustrated in Figure 5 and Figure 6. There are no return signals from the target at a distance of 1700 m.

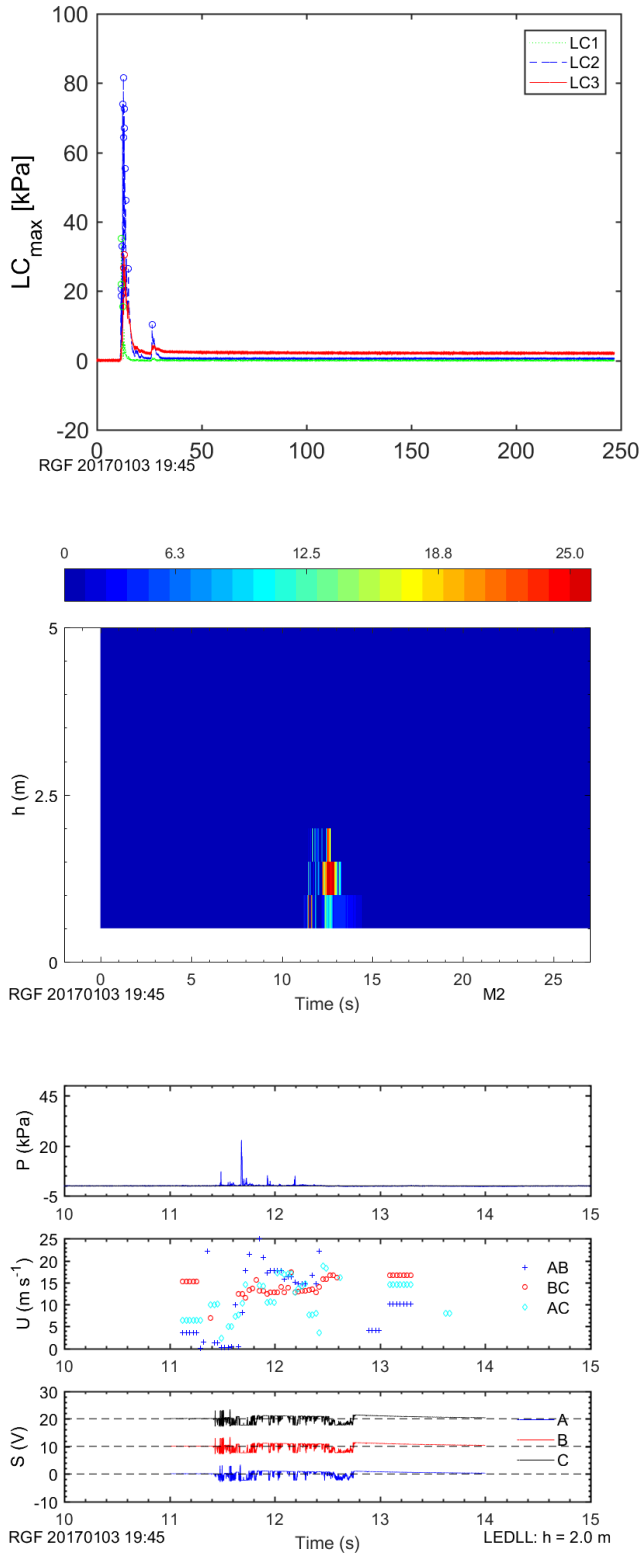

Figure 1 Natural avalanche 20170103 19:45: Pressure measurements at the concrete wedge (top) and mast 2 (middle). Pressure and velocity measurements at mast 2 (bottom)

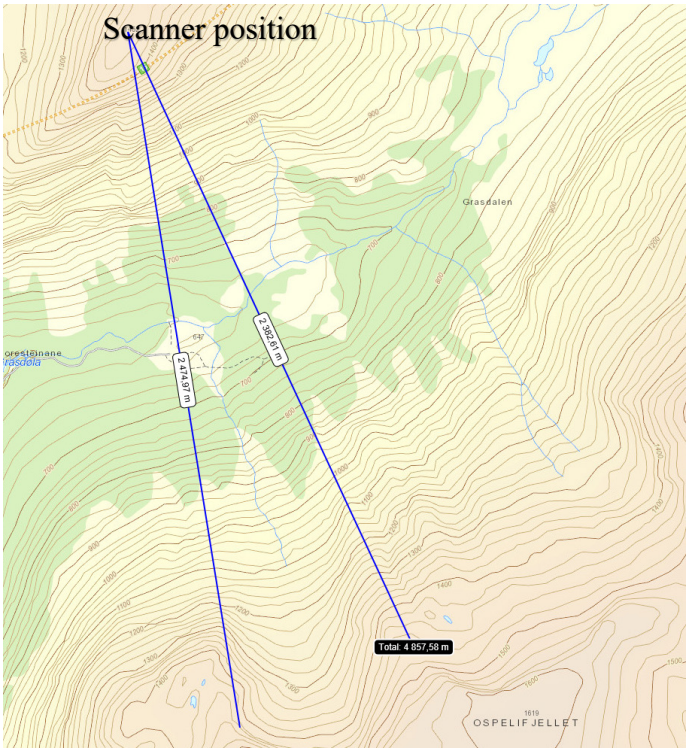

Figure 2 Map of Sætreskarsfjellet in the north with laser scanner position and Ryggfonn in the south, which was the scanning target

Figure 3 Ryggfonn seen from Sætreskarsfjellet during the campaign. Photo taken with normal camera

Figure 4 Ryggfonn seen from Sætreskarsfjellet during the campaign. Photo taken with the camera on the Optec scanner. The air appears noticeably more blurry than in Figure 3

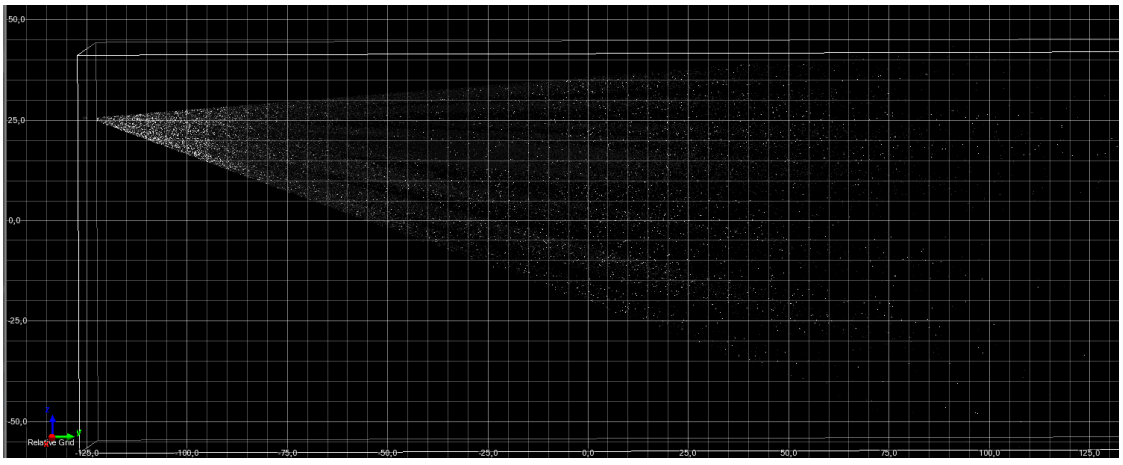

Figure 5 Result of the first scan at Ryggfonn (before the avalanche releases), with signals projected onto the vertical plane along the line of sight. The laser beam is reflected by scatterers in the air in front of the scanner. The white dots are data points.

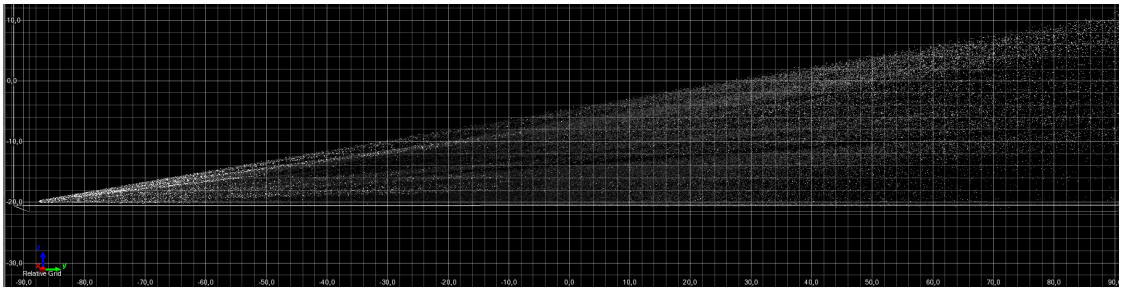

Figure 6 Result of the second scan (after the avalanche release) at Ryggfonn, with signals projected onto the vertical plane along the line of sight. Scatterers (white dots) dispersed throughout the entire air volume between the scanner and the target completely mask the latter

To verify that the scanner was working correctly, several test scans were done at Venabygdsfjellet (Ringebu municipality, Oppland County, approx. 900 m a.s.l.) some days later; see Figure 7 and Figure 11 for the locations of the scanner. The target surface was covered by snow, as it was at Ryggfonn. There was little wind and no snowdrift (Figure 8). The results from the first test scans (Figure 7–Figure 10) show convincingly that the scanner is perfectly capable of scanning snow surfaces and that it is working as expected.

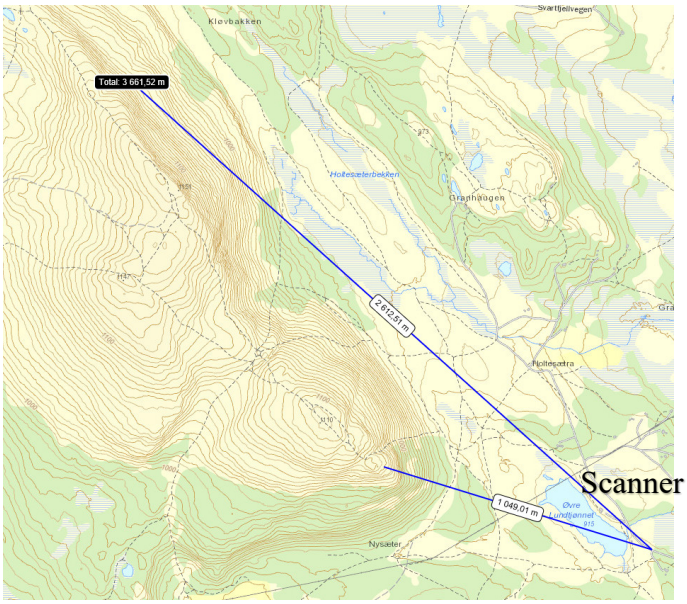

Figure 7 Scanner position and target for test scan 1 at Venabygdsfjellet

Figure 8 The weather situation when test scan 1 at Venabygdsfjellet was carried out. Good visibility, no sun and "nothing in the air"

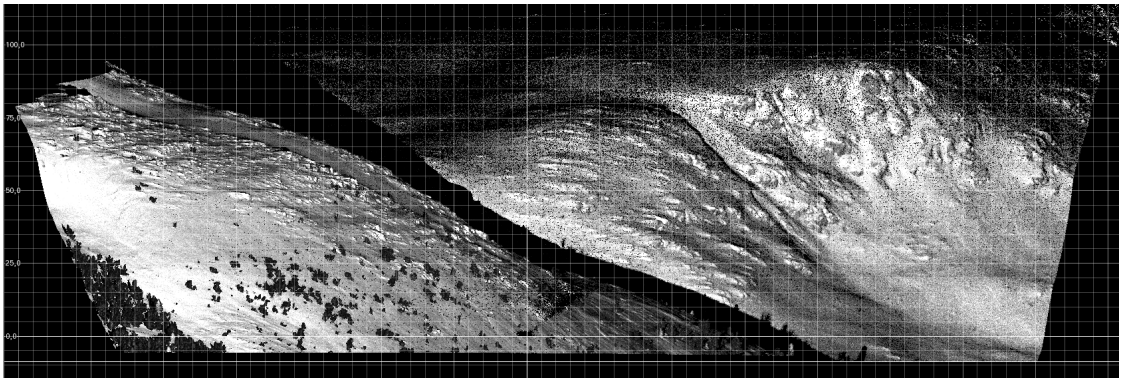

Figure 9 Result of test scan 1 at Venabygdsfjellet. The snow surface reflects the laser beam very well

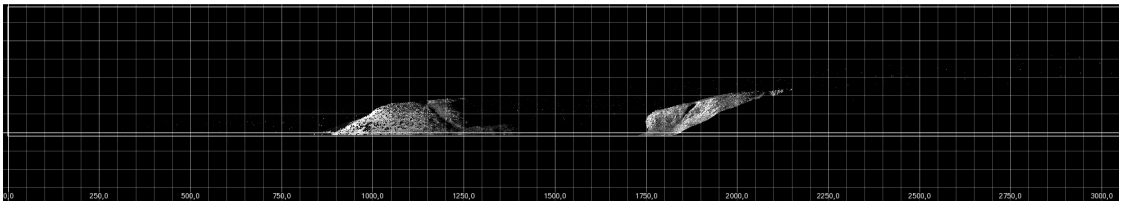

Figure 10 Result of test scan 1 at Venabygdsfjellet, with the reflections from two narrow azimuthal sectors projected onto the vertical plane along the line of sight from the scanner to the target

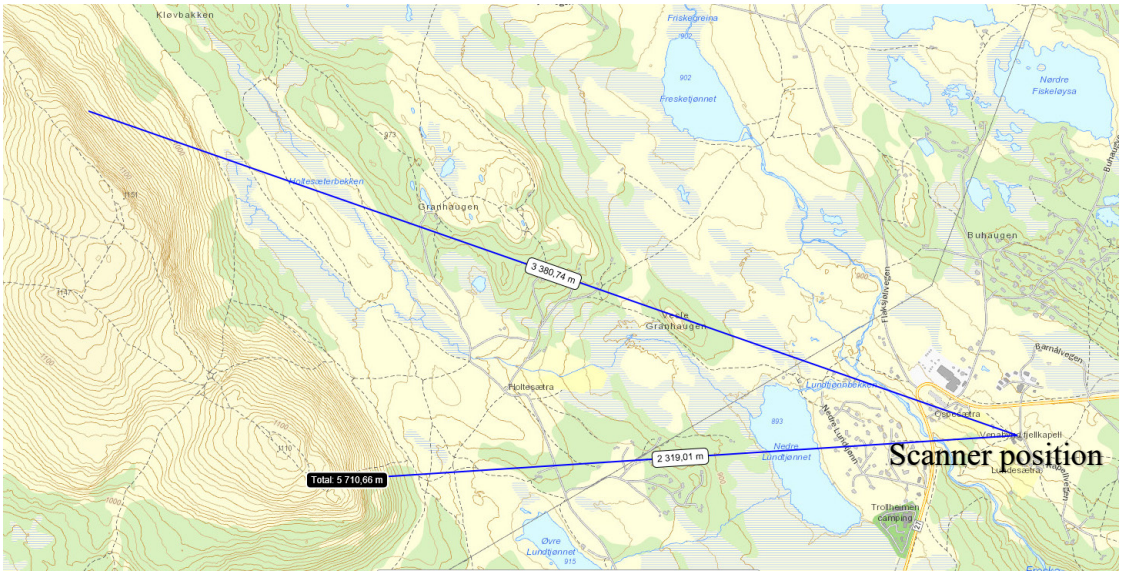

Figure 11 Map of scanner position to the right and target to the left in the second set of tests. The right-hand sector of the target is significantly farther from the scanner than the left-hand side of the target, explaining the clouds behind left side of target.

During test scan 2 from another position (Figure 11), the right-hand side of the target area was covered with clouds hanging near the mountain side on the right-hand side of the scanning area (Figure 12). The area partly covered with clouds was included in the scan to compare scanner performance in the presence of small water droplets and without. As expected, the part covered with clouds did not have any reflection from the real target, only from scattered particles in the air (Figure 14 and Figure 15).

Figure 12 Photo taken with the camera in the Optec scanner. The visibility is sufficient, except for right part of the target, which is covered by clouds

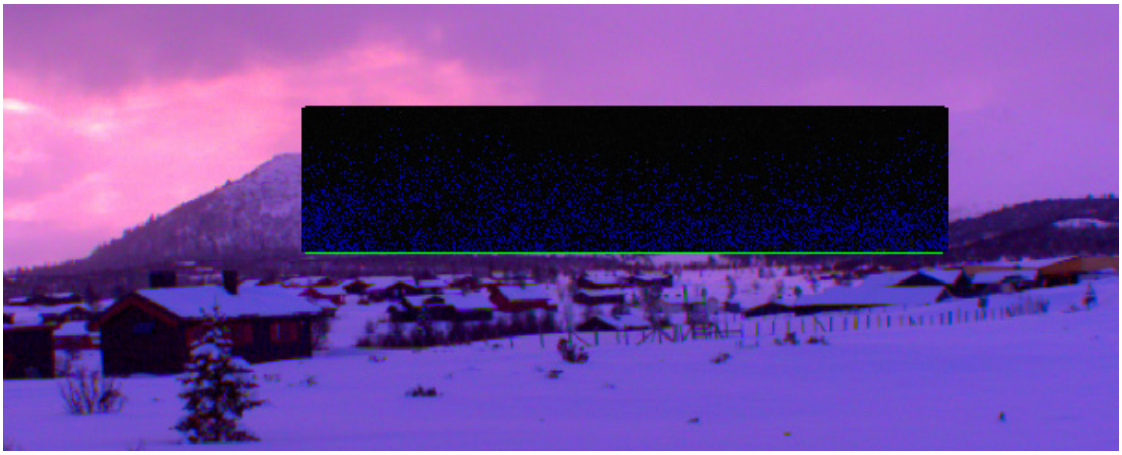

Figure 13 Photo taken with camera in Optec scanner. The inset rectangle marks the scanned area

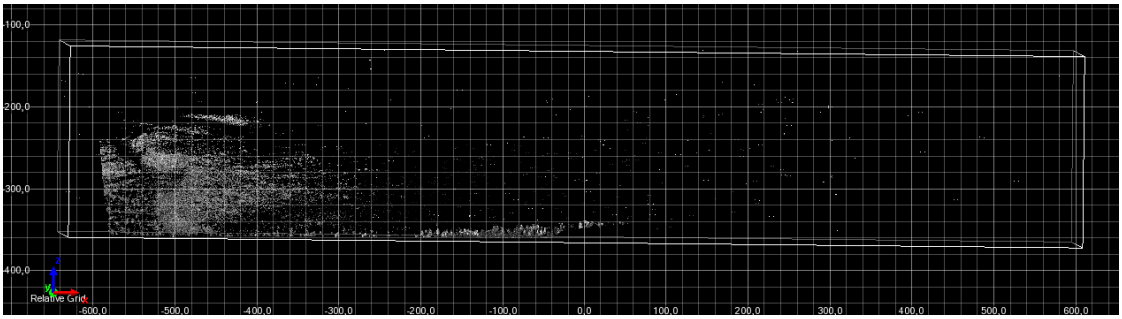

Figure 14 Result of test scan 2 projected onto a plane perpendicular to the line of sight. On the left-hand side, where there are no clouds, reflections from the snow surface are recorded, but not on the right-hand side

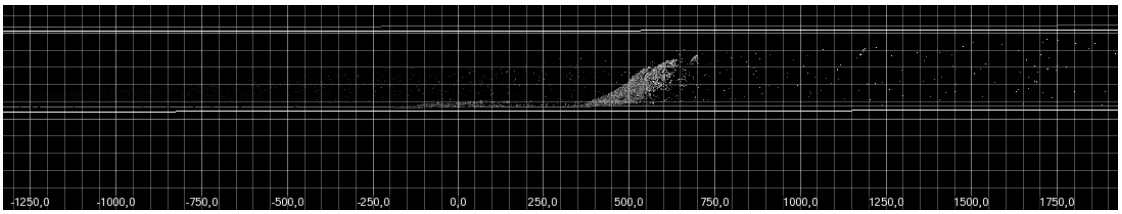

Figure 15 Result of test scan 2 seen normal to the line of sight. Noise from the cloud in front of the target area is visible as sparsely scattered dots at a larger distance from the scanner than the nearest part of the target, which is detected around coordinate 500

This finding strongly suggests that there were very small ice crystals suspended in the air on the southern side of Sætreskarsfjellet during the measurement campaign that did not scatter a significant amount of light in the visible range and thus were not visible on photos. However, in the near-infrared frequency band used by the LiDAR scanner, these

particles reflected and dispersed so strongly that the signal from the distant snow cover was completely overpowered.

The main conclusion from this experience and the subsequent tests is that LiDAR scanning of the snow-cover surface is strongly affected by the atmospheric conditions and may fail to give results in situations which otherwise are well suited to avalanche experiments. The most critical conditions seem to occur when there is fine-grained new snow at low temperatures and sufficiently strong wind to suspend the smallest particles. Such conditions are most often found at ridges where the air flow detaches from the ground and may carry the snow particles far away from the ground. At Ryggfonn, this can be the case both at Sætreskarsfjellet under winds from the sector NW to NE and at Ryggfonn under winds from the opposite sector.

2.2.3 Data analysis

In the course of 2017, the comparison of data from Ryggfonn with measurements and observations from other sites was continued (Gauer, 2017). A scaling analysis using a simple mass block model supports Observations and measurements on snow avalanches indicate that the maximum front velocity of major avalanches scales with the total drop height as $U_{\max} \sim \sqrt{gH_{\mathrm{sc}}/2}$ and mean velocity $\overline{U} \approx \frac{2}{\pi} U_{\max}$ (Gauer, 2012, 2013, 2014); here, H_{sc} is the maximum drop height, i.e., usually the altitude difference from the release area to the valley bottom. The most popular friction law in avalanche dynamics, the Voellmy friction law, is not able to reproduce this scaling behavior.

What do these experimental findings imply for avalanche dynamics? Do they have any relation to another long-established empirical finding, namely the linear dependence of the mean run-out angle $\bar{\alpha}$ on the path steepness β? In order to shed light on these questions, the motion of a block on a parabolic path was studied (Gauer, submitted). The friction acting on the mass block is assumed either as a constant retarding acceleration, a_{ret} = cst., or as Coulomb friction, $a_{\mathrm{ret}} = \mu g \cos\theta$, where θ is the local slope angle. The analysis reveals that the scaled velocity $\hat{u} = U_{\max}/\sqrt{gH_{\mathrm{sc}}/2}$ can be expressed as a function of the angles α and β in this simple setting, independent of the coefficient of the parabola or the absolute value of the drop height. Figure 16shows $\hat{u}$ as contours in the α-β parameter plane. The contour lines are almost parallel to the line representing the prediction of the α-β model, the latter corresponding to a velocity value $\hat{u} \approx 0.85$. This shows that a simple Coulomb model explains a large part of the effective friction in snow avalanches. This analysis is also consistent with an empirical probability analysis of an extensive data set of maximum frontal speeds of flowing avalanches from 36 avalanche paths (McClung and Gauer, submitted).

This analysis suggests to rephrase the fundamental questions of avalanche dynamics as follows: Why are Coulomb friction or a constant frictional deceleration so good approximations? And how can we explain the slope-angle dependence of the effective friction?

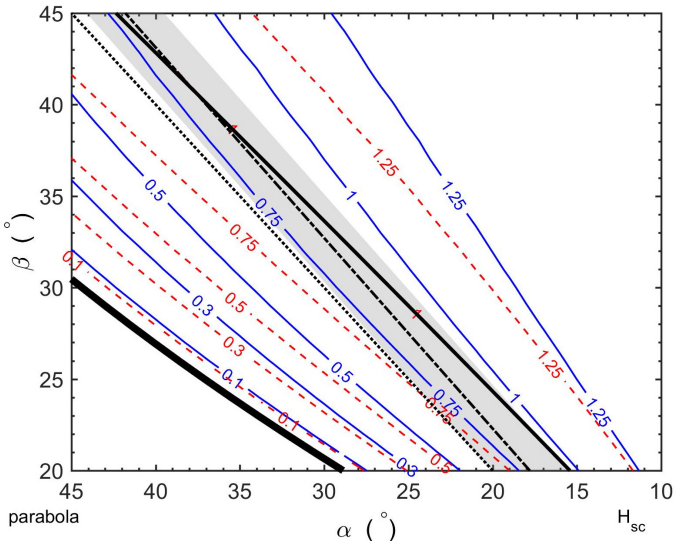

Figure 16 Contour plots of the ratio $U_{\max}/\sqrt{gH_{sc}/2}$ for a mass point moving on a parabola either with constant a_{ret} (full blue lines) or Coulomb friction (dashed red lines) in the parameter plane spanned by the runout angle α and the path steepness β. The black line inside the grey band divides avalanches stopping before the bottom of the parabola (lower left) from those stopping on the opposite slope (upper right). The thick black line corresponds to cases where the avalanche only moves infinitesimally because the friction coefficient is equal to the tangent of the slope angle in the "release area". For comparison, avalanches stopping at the β-point (dotted line $\alpha = \beta$), at the angle $\bar{\alpha}(\beta) = 0.96\beta - 2.3°$ predicted by the well-known α-β model (black dashed line) and within one standard deviation from $\bar{\alpha}(\beta)$ (gray shaded area) are also plotted in the diagram (for explanation see Lied and Bakkehøi, 1980)

2.3 Model development

A large part of the budget for 2017 was used to complete the NGI Technical Note 20140053-03-TN from the previous project period; the report was delivered together with the Annual Report 2016 (Issler, 2017a). This work focuses on the mechanism(s) responsible for fluidization of snow avalanches. In earlier work (Issler and Gauer, 2008), it was assumed that snow particle collisions—despite their inelasticity—are chiefly responsible for driving the particles farther apart as the shear rate increases. While particle collisions undoubtedly have to play a role in this process, it was already earlier found that the dispersive pressure created in this way might not be sufficient except in very steep avalanche paths, and it was conjectured that the ambient air flowing over the avalanche creates considerable suction that supports fluidization. Later on, an additional—and perhaps decisive—mechanism was recognized, namely expulsion of air from the snowpack due to the extra overburden applied by the avalanche. On the basis of the theory presented in (Issler, 2017a), implementation in a quasi-3D numerical code to test this new mechanism can be initiated as soon as funding can be secured. Some more theoretical work should, however, dedicated to the effective permeability in the case of turbulent air flow across the snow cover and the avalanche.

In a number of consulting projects, powder-snow avalanches (PSA) are important in that they determine the extent of the endangered area. The stagnation pressure of PSAs is significantly lower than that of typical dense-flow avalanches, but they may run up to several hundred meters farther than the latter. In many cases, mitigation at moderate cost may be possible by dimensioning buildings to the expected pressure. The consultant is thus confronted with the task of estimating the relevant stagnation pressure, but presently only AVAER, a center-of-mass model with variable size (Beghin and Olagne, 1991; Rapin, 1995), SL-1D, a quasi-2D two-layer model for the fluidized and suspension layers (Issler, 1998, 1999) and SAMOS-AT, a coupled quasi-3D/full-3D model for the dense and suspension layers (Sampl and Granig, 2009) are available to consultants (and partly at high cost). At NGI, SL-1D has been used occasionally despite its known weaknesses (the user has to select the path taken by the avalanche in advance, the often important lateral spreading is neglected, the two layers are not coupled to the dense-flow layer from which they originate, etc.). A method for approximatively taking into account lateral spreading as well as an extension for simulating the effect of mass and momentum loss at obstacles like dams were later developed by SL-1D's author, but never described in a publicly accessible way. To remedy this documentation gap, an NGI Technical Note (Issler, 2017b) was written, which can be distributed with consulting reports or obtained by interested outsiders.

The need for a numerical model of mixed avalanches that is well founded on up-to-date knowledge of the physical processes in such avalanches, yet is easy to use in consulting, has been widely felt. At SLF in Davos, Switzerland, Bartelt and co-workers developed several extensions to their commercial quasi-3D Voellmy-type model RAMMS::AVALANCHE (Christen et al., 2010), which is also widely used in Norway, and described them in a series of papers, most recently (Buser and Bartelt, 2015; Bartelt et al., 2016). It seems that SLF plans on merging these extensions into the commercial version soon. Therefore it seemed timely to scrutinize these models and to publish the findings in a peer-reviewed paper. Issler et al. (2017) arrive at the following main conclusions: (i) The general approach of describing avalanches as two-layer flows with variable densities (dense/fluidized and suspension layers) is a suitable concept. (ii) Using the Voellmy model as a basis and modifying its two parameters as an exponential function of granular temperature is heuristic, lacks support from the kinetic theory of granular flows and leads to implausible asymptotic behavior. (iii) There are conceptual and mathematical errors in the derivation of an evolution equation for the density in the lower layer, leading to a third-order differential equation instead of a first-order or second-order equations. Moreover, an analysis of time scales reveals that an algebraic equation would be most suitable. (iv) The equations for the suspension layer lack essential terms like gravity, disregard a wealth of established experimental knowledge about turbulent gravity-driven flows and invoke a highly speculative mechanism for generating the suspension layer from the fluidized layer. The model thus needs to be thoroughly revised before introducing it into practical use.

3 WP 2 – Statistical tools

The StatPack model is now implemented into ArcGIS and ready to be tested against historical forecasts and then used as a tool for forecasting purposes. In this section we will briefly describe the model and the current status, as well as point out some important improvements that may be done.

When running the model, the computational domain is divided into a uniform grid with a typical resolution of 10 m (or coarser). The model computes, for each cell in the grid, the probability to be hit by a snow avalanche based on both weather and snow conditions in addition to the terrain. First the model computes the avalanche triggering probability (ATP), then the distribution of run-out distances is calculated. Both the probability for triggering and the run-out distribution is computed for all computational cells in the domain (except for cells with slope angles below 23° and above 70°). Combining these quantities gives a hazard map with the probability of being hit by a snow avalanche within a given time interval (typically a day for forecasting).

3.1 Triggering probability

The triggering probability is based on

- Forecasted (f) weather conditions
  - Temperature (fT)
  - Change of temperature next 24 hours (fdT_24)
  - Wind speed next 24 hours (fFF_24)
  - Wind direction next 24 hours (fDD_24)
  - Precipitation next 24 hours (fRR_24)
- Observed (o) weather conditions
  - Precipitation last 24 hours (oRR_24)
  - Snow height (oSA)
  - Change in snow height last 24 hours (odSA_24)

In addition, we also include a parameter for describing the probability of a persistent weak layer (PWL).

Traditionally, ATP is indirectly assessed by snow avalanche forecasters (experts) while they conclude upon snowpack stability at the moment and upon its change during the forecasting period based on their personal judgement, knowledge and experience. In the forecasters' decision making, a considerable role is played by the recent meteorological history of the area the forecast is produced for, as well as by forecasted weather development.

In the statistical model, we apply an approach based on fuzzy inference to estimate ATP through the quantitative parametrization of expert judgement. This approach is able to model complex systems and replicate human expert information and reasoning. Without going into details, we end up with a database for the ATP, with a given value of the ATP

for each combination of the parameters listed above and for each cell in the computational domain.

3.2 Probability distribution of run-out

The conditional probability distribution of being hit at a given point (provided that an avalanche is triggered) is based on the alpha-beta method, see Figure 17. The statistics applied for the run-out calculations in the model is based on the source database for a set of avalanche paths for large Norwegian snow avalanches (~ 200 avalanches).

The slide path from a given cell is determined by applying a simple approach letting the path follow the steepest direction (out of eight possible) from a cell to the next.

The alpha-beta model (Figure 17) is expressed probabilistically as

$$\alpha_{\text{prob}} = \alpha_{\text{det}} \cdot \varepsilon,$$

in which α_{det} is a deterministic analytical model and ε is a multiplicative model factor, giving the distribution of α_{prob} around α_{det}. The probability density of the model factor ε is calculated from the source database and shown in Figure 18. A linear function is selected as deterministic model:

$$\alpha_{\text{det}} = p_1 + p_2 \cdot \beta.$$

Estimators for the deterministic coefficients for the linear model are obtained by least-squares regression of the source database: $p_1 = -0.60$ and $p_2 = 0.91$. These factors differ from the traditional alpha-beta model values (Lied and Bakkehøi, 1980) because some events in the database were filtered out after revisiting the available information on each event. The deterministic model is plotted in Figure 19, together with the source data points.

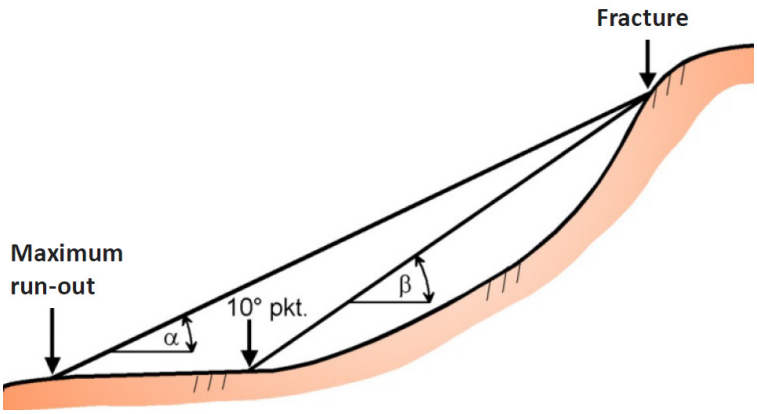

Figure 17 The alpha-beta method

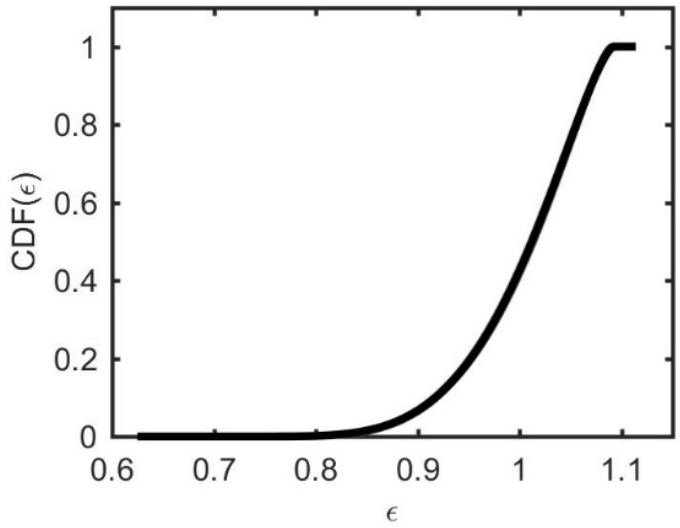

Figure 18 Probability density of the model factor ε

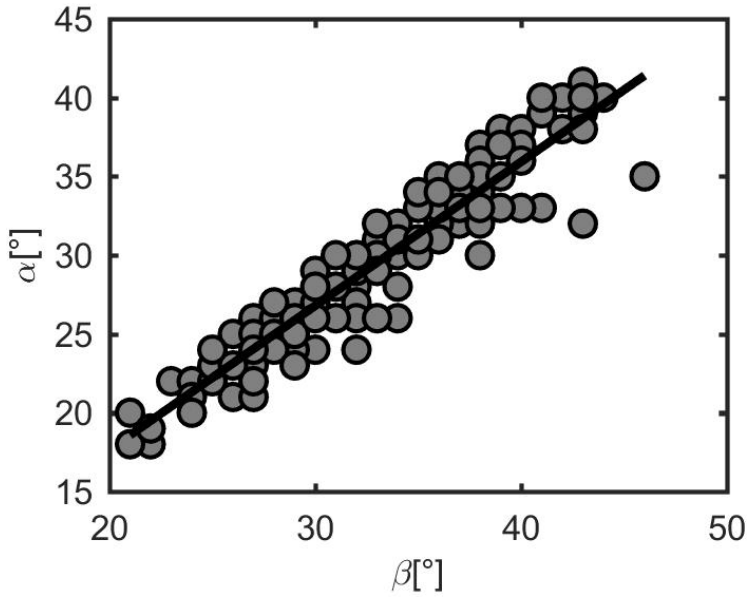

Figure 19 Deterministic alpha-beta model (black line) derived from the data from the avalanche database (dots)

3.3 The algorithm, step by step

1. The computational domain is divided into a uniformly spaced grid with a given resolution.
2. From each computational cell
    a. A slide path is defined and α_{det} is determined.

b. The distribution of the conditional probability to be hit along the slide path given a triggering from the source cell is then calculated.
c. The ATP for the actual cell is extracted.
d. The probability to be hit along the slide path given the weather/snow conditions and terrain (given as input) is then found by multiplying the corresponding values from points 3.b and 3.c.
e. The hazard map for the entire computational domain is then updated for values of the impacted cells from point 3.d if the impact probability is larger than the previous value at that location (see Figure 21 for an example).

3.4 Implementation of the program package

StatPack exists both in a pure Python version and now also as an application in ArcGIS. The latter version makes the extraction of DEMs easy, and is integrated into the same workflow as other tools and models at NGI. The interface is shown in Figure 20.

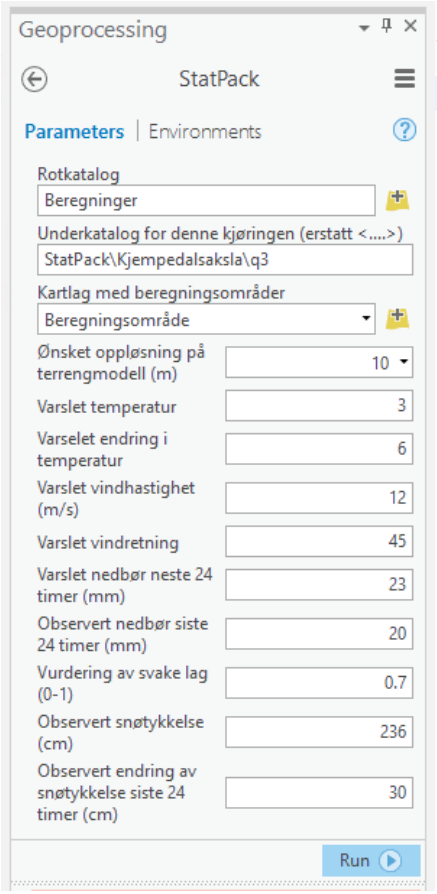

Figure 20 Dialog box for running StatPack within ArcGIS

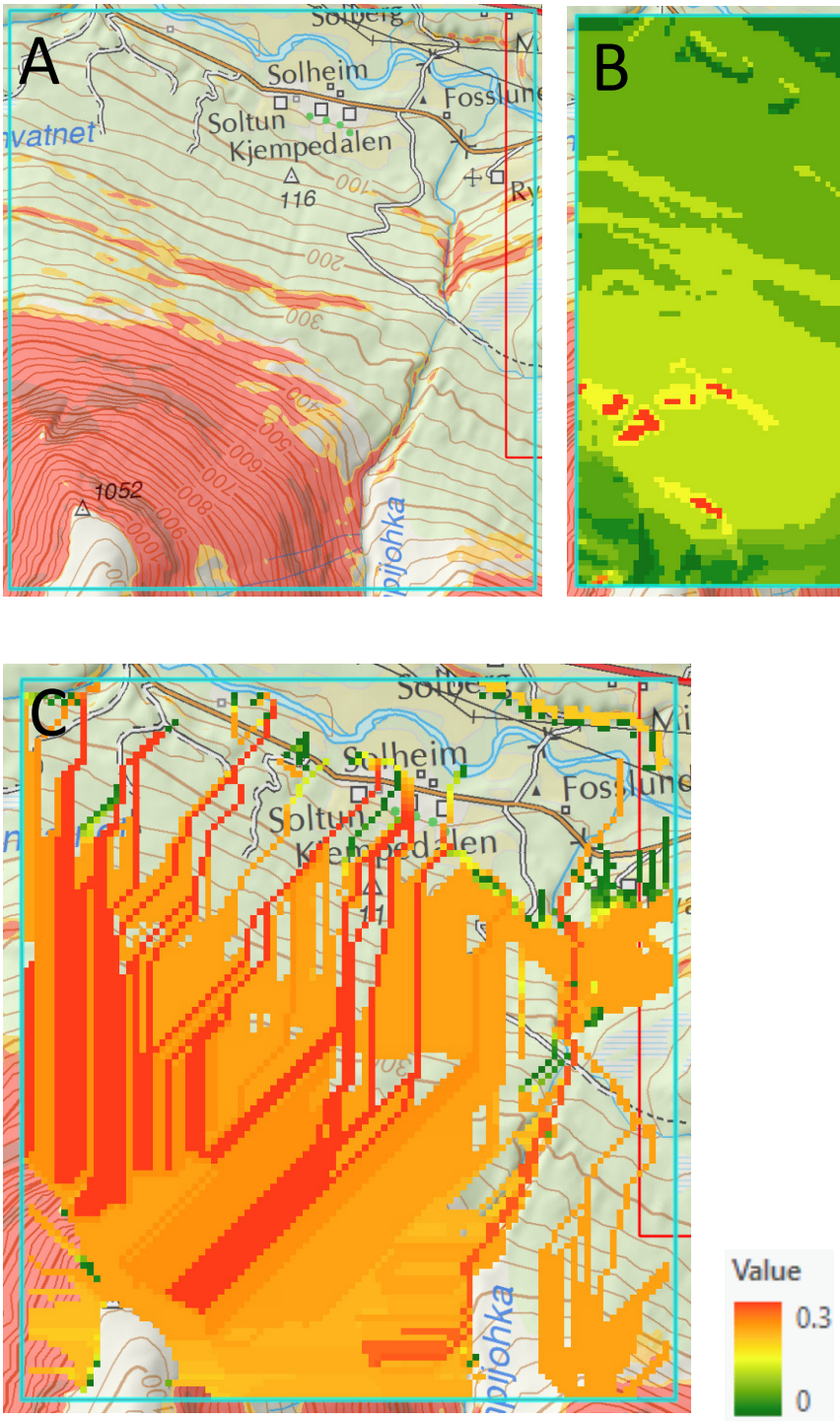

Figure 21 The digital elevation model (DEM, A), the avalanche triggering probability (ATP, B) and the probability for being impacted (C). In the DEM, yellow, red and brown areas correspond to terrain inclinations in the ranges 27–30°, 30–45° and 45–60°, respectively

3.5 First tests and planned improvements

Figure 21 shows an example of running StatPack at the mountain Stortinden, close to Nordkjosbotn in Troms County (northern Norway). For the assumed nivo-meteorological situation, the ATP ranges from 0.15 to 0.26 (within the next 24 hours). The parameters that are dependent on the DEM and give a variation of the ATP are the slope angle and the wind direction (relative to terrain).

From the maps B and C, a number of issues can be identified:

- Compared to the "true" release areas, the ATP is evaluated as only a factor 2 lower in terrain where, in reality, avalanches cannot be released at all. This indicates that the parameterization of some of the fuzzy membership functions need to be adjusted substantially, in particular with regard to the slope-angle dependence.
- Due to the rectangular grid, the StatPack avalanches can move only along the coordinate directions or the diagonals. This may lead to substantially wrong flow paths in the case of long run-out.
- There is a strong tendency for the simulated avalanches to concentrate in gullies, even though the gullies may be much too small to contain the run-off of a real avalanche. In contrast, the areas between gullies may be indicated as completely safe whereas, in reality, the impact probability is essentially the same as in the gully.
- A less conspicuous weakness is that all cells from which a release can originate are treated as part of a single release area. For each cell, only the maximum impact probability for all avalanche trajectories that hit this cell is retained. In reality, however, several distinct release areas may have trajectories through the same cell, thus those probabilities should be suitably added (taking into account possible correlations.

In order to remedy these shortcomings, the following further developments and modifications are planned:

- The fuzzy membership functions will be reviewed and modified in order to take the effect of slope angle on shear stress in the weak layer into account.
- A modified avalanche propagation algorithm will be tested that allows the avalanche to deviate from the path of steepest descent stochastically, with the deviation probability weighted by the difference in steepness between different directions.
- The maximum impact probability at a cell will be computed separately for each *connected* release area and the corresponding probabilities added (possibly taking into account correlations between releases in distinct release areas).

4 WP 3 – Slushflows

4.1 Snow cover simulations

Work has been done on the applicability of different atmospheric stability approaches in the SNOWPACK model (Jordet, 2017). The results show that the choice of parameterization has significant impact on the model results. Tests against observed snow profiles from the Grasdalen experimental site show that the best agreement between observed snow properties and model results can be reached by applying the neutral Monin–Obukhov (MO) mode of the SNOWPACK model. The study also shows that the choice of atmospheric stability model does not accommodate the observed snow properties for the entire season. While the neutral MO mode produces good results in mid-winter, it shows problems with reproducing the melting period in spring (Figure 22). Vice versa, the MO and Richardson models fit better in the melting period, but fail mid-winter. This indicates that there is a need to adjust the parameterization of the model to the actual atmospheric conditions rather than to choose one fixed model for the entire winter season. The study by Jordet (2017) also showed that radiation measurements are essential to achieve realistic results in snow pack modelling.

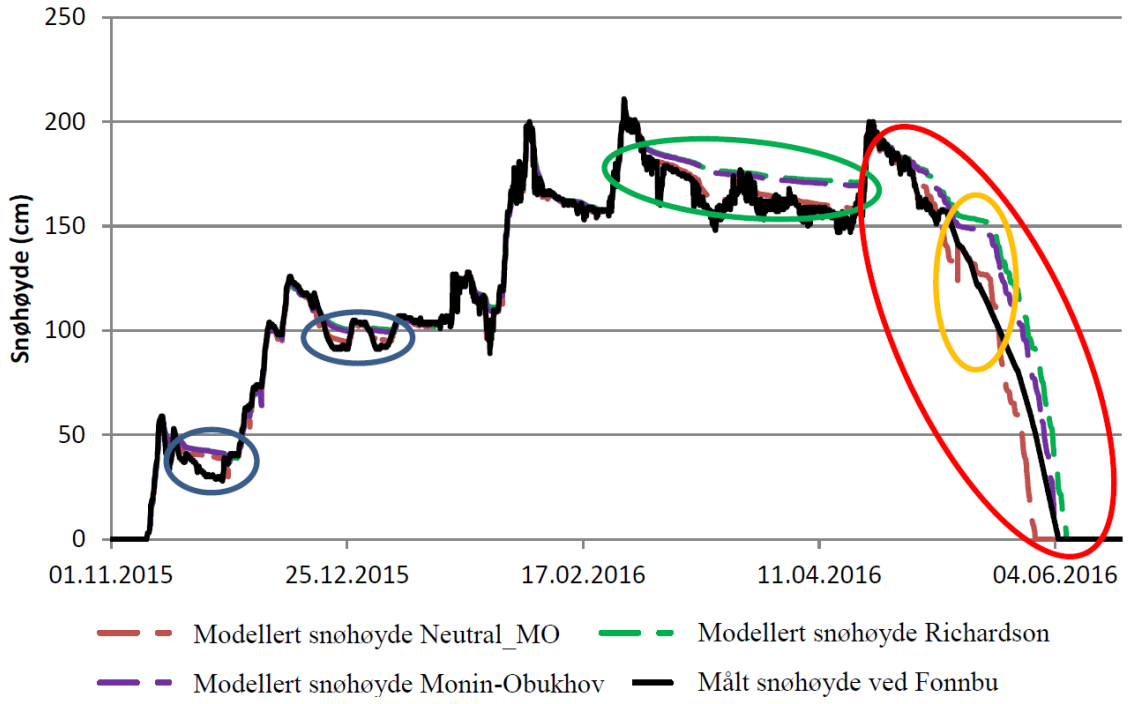

Figure 22 Measured and modelled snow height at the Fonnbu station. Blue circles show shorter periods where modelled snow height is higher than measured. The green circle shows a longer period with the same deviation. The red circle shows the melting period where deviations between model and observations is biggest. Orange circle shows the largest deviations in May

For 2018 the implementation of an automatic routine to produce hourly SNOWPACK results will be implemented.

4.2 Dynamical simulations of slushflows

This activity will take place in 2018.

4.3 Circum-Arctic Slushflow Network (CASN)

The Circum-Arctic Slushflow Network has the aim to gather researchers and practitioners that are interested in, and working with, all aspects of slushflows. The network should discuss current interests and research on the subject, support cooperation and suggest common guidelines for managing slushflow hazards and risks.

After a constitutional meeting at the ISSW 2016, the network has established a homepage and keeps frequently contact to interested members. The level of activity can certainly be higher since there is an increasing interest in the subject of slushflows.

The new homepage includes a general description of the slushflow phenomenon and its occurrence, an extensive list of publications on slushflows, and observation guidelines for slushflow events. There is also the ambition to collect documentation and links to pictures and reports on interesting slushflows in the northern hemisphere.

In 2017 a major advance was made when NVE and NGI co-organized a slushflow workshop in Oslo in November 2017, following up on an initiative by the avalanche group of the Icelandic Meteorological Office. Researchers and practitioners from Norway, Iceland and Greenland participated in the seminar (Figure 23). During day one, the situation in each country and ongoing research was presented. During day two, a smaller group discussed possibilities for cooperation in slushflow forecasting in Norway and Iceland.

Figure 23 Slushflow workshop at NVE headquarters, November 2017

5 WP 4 – Investigation of relevant snow avalanche events

5.1 The 2017-01-18 avalanche at Rigopiano, municipality of Farindola, central Italy

Strong Bora winds from Russia that picked up large quantities of humidity across the Adriatic Sea caused intensive snowfalls on the on the eastern slope of the Apennine in mid-January. Even below 1000 m a.s.l., snow depths of 2 m and more were recorded. Apparently, the winds were not very strong even across the crest line in the Gran Sasso area west of Pescara, so that the even larger quantities of snow at altitudes near 2000 m a.s.l. were deposited on the east-facing slopes. In the afternoon of January 18, 2017—just hours after a series of substantial earthquakes in the area—a large avalanche released near the summit of Monte Siella in the municipality of Farindola (province Pescara, region Abruzzo), descended the Grave Bruciata channel and annihilated the four-story luxury hotel Rigopiano, after completely breaking and largely entraining a more than 70 years old stand of beech trees over a distance exceeding 1 km.

While two persons happened to be outside at the east side of the hotel, 38 guests and employees were waiting inside for evacuation when the avalanche struck. The chaos due to the earthquakes, the deep snow on the roads, avalanches that had crossed the access road, persistent bad weather conditions and the complete collapse of the large building made the rescue operations unusually difficult and time-consuming. Of the nine survivors inside the building, the last were liberated after four days; they all survived thanks to being farthest away from the centerline of the avalanche. After a week, all 29 victims were found. In terms of deaths, this was the third-deadliest avalanche in Europe after the catastrophes in Austria in early 1954.

On the scientific side, several aspects of this avalanche event are of interest: What can we learn about the braking effect of the forest? Why was this avalanche able to utterly destroy a fairly new building so far out in the run-out zone? What can be learnt about the vulnerability of people inside buildings? Would our present best-practice avalanche hazard mapping procedures have been able to recognize the danger? In order to search for answers to these questions, D. Issler visited the site during a private visit to Italy in early June. Due to the ongoing legal investigations of the accident, a fairly large area around the hotel was closed off. It was, however, possible to reach the avalanche path by foot and to descend it from the release area to the upper run-out zone. Information about the construction of the hotel and its failure modes could thus not be gathered, but the necessary detour in approaching the avalanche path revealed that avalanches had also released in two neighboring paths, with considerable forest damage.

A detailed report on the findings from the field work and on the interpretation of information gathered on the Internet will be completed soon. The gathered data should allow

to set the initial and boundary conditions for numerical simulations with a Voellmy-type model that includes the extra friction and drag due to the forest (Issler, 2016).

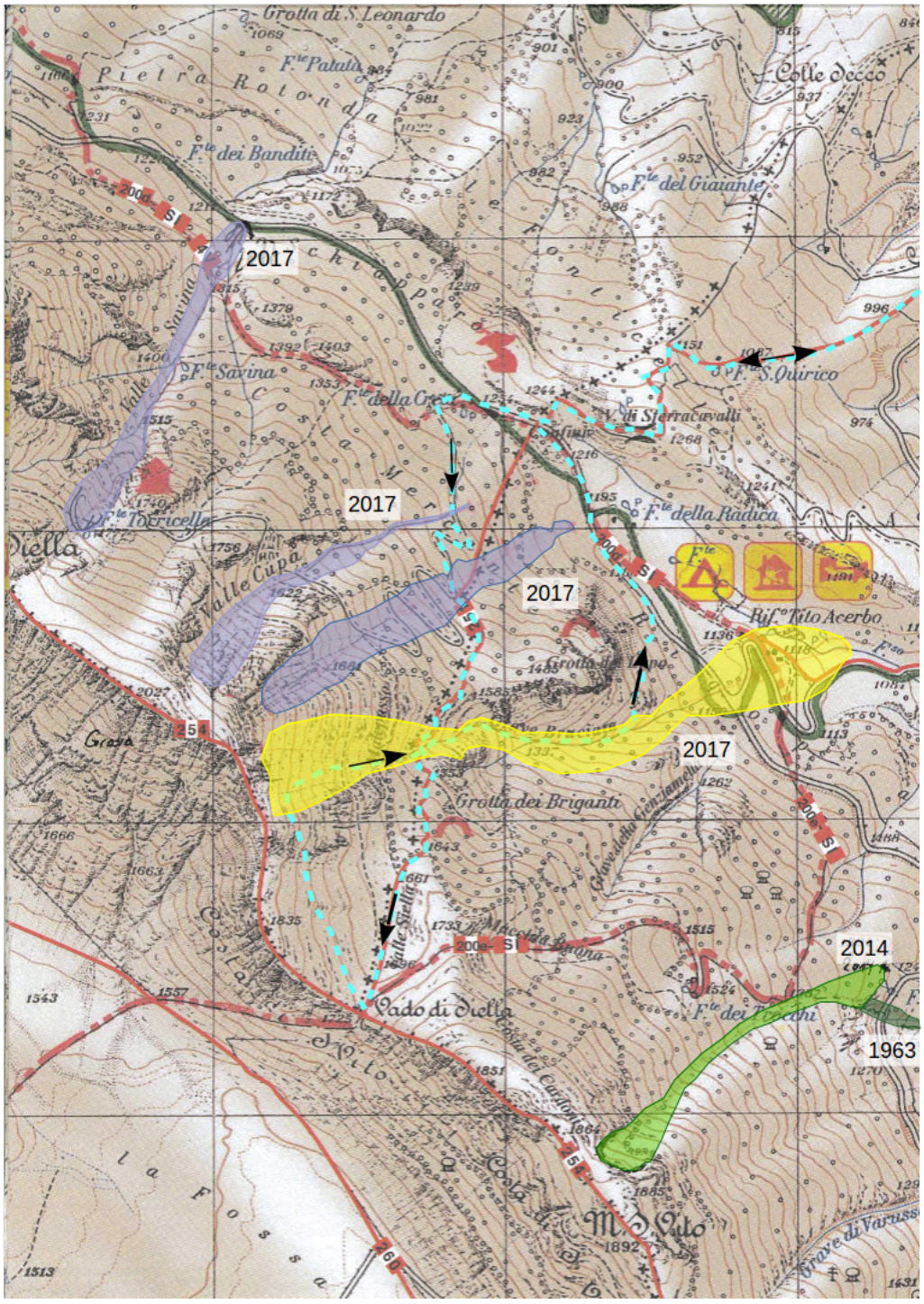

Figure 24 Map of the 2017 Rigopiano avalanche and some known avalanche events nearby. Survey path indicated in cyan and with arrows. The coordinate lines have a spacing of 1 km

Some of the main points can be summarized as follows:

- The avalanche had both high-speed and moderate-speed components, which followed different paths at the bends.
- Due to the rather shallow humus layer, the beech trees were mostly uprooted, but some were broken at 0.5–1.5 m above the ground, i.e., close to the snow surface.
- The broken or uprooted trees seem to have been transported over considerable distances, but in most cases presumably not exceeding a few hundred meters.
- The data on victims and survivors complements the data from the 2015 Longyearbyen avalanche and helps to define the lethality curve as a function of the structural damage of the building (see Figure 25).
- Avalanches are much more frequent in this area of the Apennine than one might think at first, given the southerly location close to Rome. Based on records of earlier events that became known after the disaster, the return period of events of this magnitude may be below 100 years. Forest damage in neighboring paths indicates that smaller avalanches have frequencies of 0.1 y^{-1} or higher.
- With a careful site investigation and by collecting historical information from knowledgeable local residents according to best practice in Norway or Switzerland, the potential of this path to release major avalanches would almost certainly have been recognized. Model calculations taking into account the local snow-climate conditions would confirm this conclusion. The critical point in the assessment would be the treatment of the braking effect of the rather dense beech forest—if it is overestimated, the location of the hotel might have been misjudged to be safe.

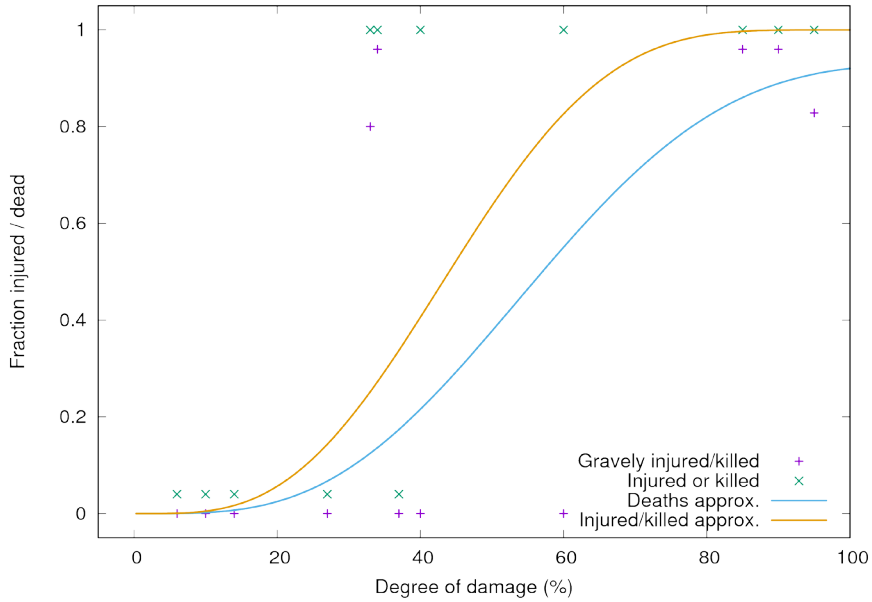

Figure 25 Preliminary vulnerability curves for death and injury inside a building as a function of degree of building damage according to (Issler et al., 2016), based on data from the 2015-12-19 Longyearbyen and 2017-01-18 Rigopiano avalanches

5.2 The 2017-02-21 avalanche at Longyearbyen

A little more than a year after the deadly avalanche that struck the well-known "spiss-hus" of Longyearbyen in December 2015, another snow avalanche released from the same mountainside a little further upstream. It damaged two houses to the point that they had to be demolished, but fortunately they were not inhabited at this point, and nobody was hurt.

NGI was called by NVE to participate in a task force investigating a number of questions surrounding this avalanche event. In this way, first-hand information on the avalanche and its effect on the buildings could be collected. The avalanche did not have features that would make it particularly interesting with regard to avalanche dynamics, except for the effect of the impact on the buildings. A modest amount of funding from SP 4 FoU Snøskred was used to collect and organize photos and other data that might be useful for research on the interaction of avalanches with structures, but no work on this topic was carried out and no formal report was written during the reporting period.

As in 2015, the avalanche was fluidized to a considerable degree and had developed a powder-snow cloud, as the snow plastered on the houses in the right half of Figure 26 (top) and the texture of the snow-cover surface show. There was considerable structural damage to the two houses that were hit hardest, but again the poor connection to the foundation led to one of them being rotated away from the other by some 30°. Interest-ingly, some of the ground-floor windows facing the avalanche were not damaged whereas the wood panels below them were utterly destroyed and significant quantities of snow invaded the building. In contrast, the wooden studs sustained the pressure with-out being broken (Figure 26, lower panel). This suggests that the flow depth of the flu-idized layer of this avalanche was hardly more than 1 m at the location of the houses and the pressure was not high. It was sufficient, though, to carry heavy objects like an all-terrain vehicle and large containers over distances of up to 50 m.

5.3 The 2017-03-15 avalanche at Haugastøl, municipality of Hol (Buskerud County)

A group of six German ski tourists skiing on gently inclined terrain at the eastern foot of Gråskallen (1289 m a.s.l.), some 7 km northwest of Haugastøl on the Hardangervidda, remotely released an avalanche that attained a maximum width of about 200 m and a length of approx. 350 m, with a fall height of 190 m. The release volume is estimated to about 10,000 m^3. All six skiers were hit by the avalanche: A 16 year old girl was buried at a depth of approx. 1.5 m, three persons were also completely buried, but with an arm or a ski pole visible. The rearmost person, buried to the knees, could free himself with his shovel, then free another person buried to the hips. Together they dug out three others who were not injured despite their complete burial. An avalanche dog found the girl after four hours. Very surprisingly, she was conscious despite not having had a breathing space around her head and having been cooled down for four hours.

Figure 26 Avalanche in Longyearbyen, 2017-02-21: View of the damage area from above (top) and detail of the damage on the rotated house (bottom). Photo C. Jaedicke (NGI)

The field survey carried out by Kjetil Brattlien (NGI) five days after the accident confirmed the accuracy of the regional avalanche bulletin for the day of the accident (danger level 3 – considerable due to snowdrift and a persistent weak layer, with high probability for remote triggering). The findings are summarized in the report (Brattlien, 2017), which also contains a description of the rescue operation and an assessment of the safety precautions that could have helped prevent this accident.

An interesting and highly pertinent observation was that this avalanche consisted of two distinct surges, the second arriving a few seconds after the first. The first surge had quite low density; according to one of the eye witnesses it clearly was not a powder-snow cloud. The girl was buried by the first surge. The second surge had higher density and overlaid the deposits of the first surge around the location of the buried girl. Apparently, the permeability of the deposits of the first surge was high enough—despite the weight of the denser deposits over it—that the girl could breathe sufficiently.

From the point of view of avalanche dynamics, these observations provide rather strong evidence for an intermediate-density, *fluidized*, flow regime in snow avalanches. It occurs at the front of the flow and is typically characterized by substantially higher velocity than the dense flow following it. Experimental and observational evidence for fluidization has been accumulating since the 1980s (Schaerer and Salway, 1980; Shimizu et al., 1980; Salm and Gubler, 1985; Issler et al., 1996; Schaer and Issler, 2001; Issler et al., 2008; Gauer et al., 2008), but only a few attempts have been made to include it in avalanche models (Salm and Gubler, 1985; Gubler, 1989; Issler and Gauer, 2008; Buser and Bartelt, 2015; Rauter et al., 2016). As emphasized by (Issler et al., 2008), even the front of quite small avalanches can attain fluidization after a short distance. In the present case, this has been the case already after a travel distance of about 100 m if the release area comprised all steep terrain down to 1160 m a.s.l. or after 200 m if only the uppermost steep area (down to 1200–1220 m a.s.l.) released initially.

Furthermore, the observed separation of the avalanche into two surges testifies to a substantial velocity difference between the fluidized front and the non-fluidized avalanche body. Only qualitative data is available, but it seems to be consistent with a front velocity of 20–25 m/s and a body velocity about half as large, as suggested by other indirect observations (Issler et al., 2008).

A day before the accident, there had been a snowfall of about 0.5 m with strong winds. When the ski tourists were taken by the avalanche, it was snowing again with an intensity of 5–10 cm/h, but the new snow was humid and cohesive. Usually, fluidized snow avalanches are observed when the snow is fine-grained and cold, with little cohesion and low shear strength. The snow from the day before meets these conditions, but not the newest snow. One may conjecture that the air temperature rose rapidly some time before the avalanche release, but only a small amount of humid snow had fallen by then. Further such observations will be useful to constrain future models based on the mechanism of fluidization by air expulsion from the snow cover under compression (Issler, 2017a).

Figure 27 The slope of the Haugastøl avalanche on 2017-03-15, the red ellipse marking the location where the buried person was found. Photo taken by the Police and Norwegian Air Ambulance on 2017-03-18

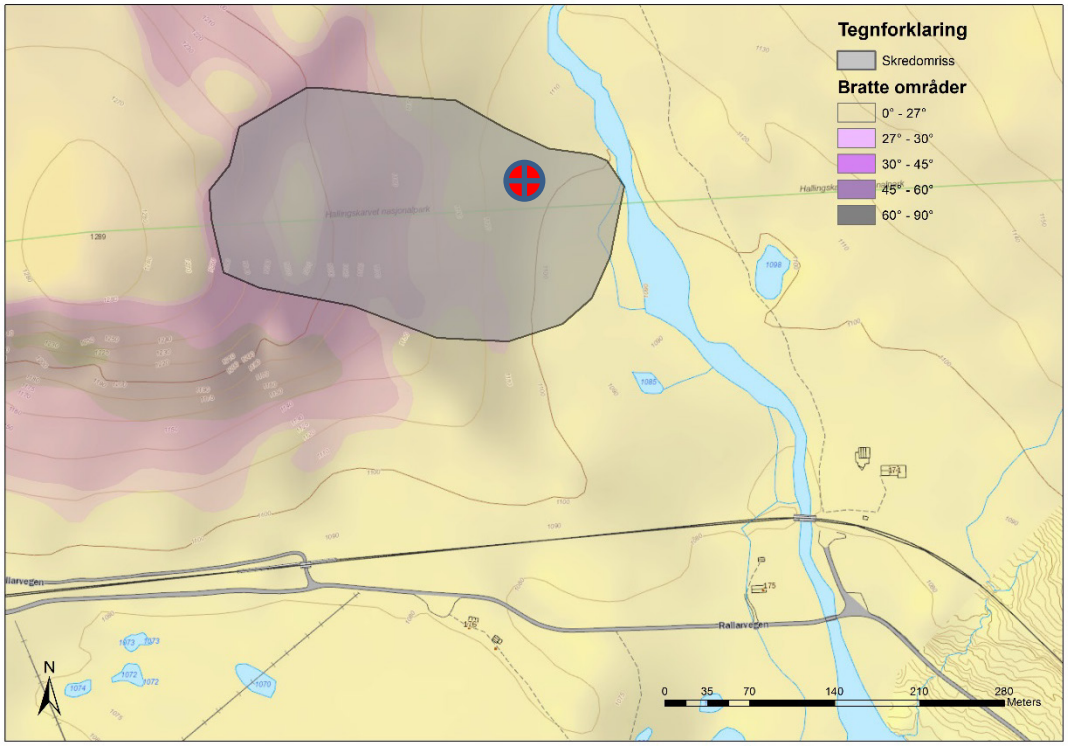

Figure 28 Map of the Haugastøl avalanche with area affected by the avalanche, terrain inclination and burial location. From (Brattlien, 2017)

5.4 The infrasound project

One of the greatest challenges for local avalanche forecasting is the availability of near real time feedback about the avalanche activity (Schweizer and van Herwijnen, 2013). Feedback and continuous updating on avalanche activity is important for learning and prediction skill cultivation in local avalanche forecasting programs (Kristensen, 2016), especially when forecasting is viewed as a Bayesian process. Avalanche activity in neighbouring paths ("indicator avalanches") provide invaluable information about the current snow stability conditions. Reliable systems for automatic monitoring of avalanche activity that can eliminate the need for visual observations, which are often hampered by darkness and weather conditions, are therefore seen as highly desirable, both for verification of the forecasts and for the operational forecasting work.

For these reasons an infrasound avalanche detection system was installed in Grasdalen in October 2014 by the Norwegian Public Roads Administration (NPRA) to test the feasibility of continuous avalanche monitoring.

The system used, called "Infra-sound Detection of Avalanches" (IDA), is based on technology developed by iTem and Laboratorio di Geofisica Sperimentale of the University of Florence, Italy (Ulivieri et al., 2012). The system is commercialized in Norway by Wyssen Norge AS, which is a subsidiary of Wyssen Avalanche Control AG in Switzerland.

5.4.1 Season 2016–2017

The NPRA had initially decided to discontinue the monitoring program in Grasdalen after the 2015–2016 season and to remove the infrasound detection system. Following a proposal from NGI to share the costs of operation, it was decided to continue the research program for two more seasons. The participants in this project are listed in Table 4.

Table 4 Participants in the testing of IDA in Grasdalen during the winter 2016–2017

Organisation	Contacts
NGI	Peter Gauer Krister Kristensen Arne Digernes
Norwegian Public Roads Administration NPRA	Tore Humstad Halgeir Dahle Martin Venås Knut Inge Orset
iTem srl Geophysics/Laboratorio di Geofisica Sperimentale of University of Florence	Giacomo Ulivieri Dario Delledonne
Norwegian University of Science and Technology NTNU	Sondre Lunde
Wyssen Norge AS / Wyssen Avalanche Control AG	Stian Langeland Cesar Vera

5.4.2 Results 2017

- Data collection throughout the winter related to the reliability of the system based on alternative sources. These include visual observations, a summit webcam at Kvitenova, a camera at NGI's research station and the monitoring system at the Ryggfonn avalanche test site.
- Throughout the winter, the system provided the NGI forecasting group with SMS and e-mail alerts, which were used operationally.
- Sondre Lunde at NTNU used data from the project for a MSc thesis on the integration of automatic alerts with the observational data management system for the regional forecasting service regObs.

During the fall, the system was moved to a location further up the valley because of better relevance to the forecasting operation and easier visual observations. The detection system was modified by Wyssen with five new sensors, better sound insulation and improved GPS equipment.

5.4.3 Plans for 2018

- Running the monitoring program through the winter season, with integration with the regional forecasting data management system regObs and the local forecasting program operated by NGI
- Analysis of the data collected during the winters 2016–2017 and 2017–2018
- Evaluation of the function and reliability of the system
- Evaluation of the utility of the monitoring program for the operational forecasting programs (at regional and local level)
- Publication of the project results in a scientific journal

6 WP 5 – Improved tools for local avalanche forecasting

6.1 Access and analysis of climatic data from SeNorge.no

The groundwork for performing data analysis of the SeNorge data has been laid. Data from SeNorge for the entire period 1957–2015, in 1 km spatial and 24 h temporal resolution, has been transferred to NGI's internal servers. Furthermore, the data has been converted to netCDF format for efficient lookup and readout of time series for arbitrary locations. Through this, a unique and pre-existing data set covering several meteorological variables has been made readily available for study and analysis. The data set covers temperature and precipitation (as interpolated variables) as well as snow accumulation, snow height and snow water equivalent (derived from precipitation and temperature through modelling).

Selected normal values have been computed for the periods 1961–1990, 1971–2000 and 1981–2010 based on this data set, namely: yearly mean temperature, winter temperature, summer temperature, monthly mean temperature, yearly precipitation and yearly maximum snow height. Additionally, the data set has been used to compute the extreme value distributions for yearly maximum snow heights, applying Gumbel distributions. Values for return periods of 10, 20, 50, 100, 300, 500 and 1000 years have been computed for all of Norway.

An application has been built to compute statistical variables and visualize these in MATLAB (see Figure 29 for an example from Fonnbu). Using the peak-over-threshold method, this has been used to obtain an extreme value distribution for 3-day and 5-day snow accumulation. The method has been tested for a sample of different locations in different climatic zones, and the correlation between extreme values and an adapted extreme value distribution has been verified as good in a majority of the cases. Extreme values are always plotted over the adapted distribution, so that correlation to underlying data can be evaluated in each individual case where this is used.

6.2 Access and analysis of KliNoGrid-data

KliNoGrid is a new product from MET consisting of gridded wind data (wind speed and direction at 10 m above ground) based on NORA10, scaled down to a grid matching the SeNorge data sets. The wind data is given with 1 h temporal resolution for the period 1957–2015. Together with precipitation and snow data from SeNorge, this can be used to indicate the dominating precipitation-carrying wind direction for any given location. This is of particular use in areas where meteorological observations are scarce. Our intention is to further use this as input to different wind schemes/models.

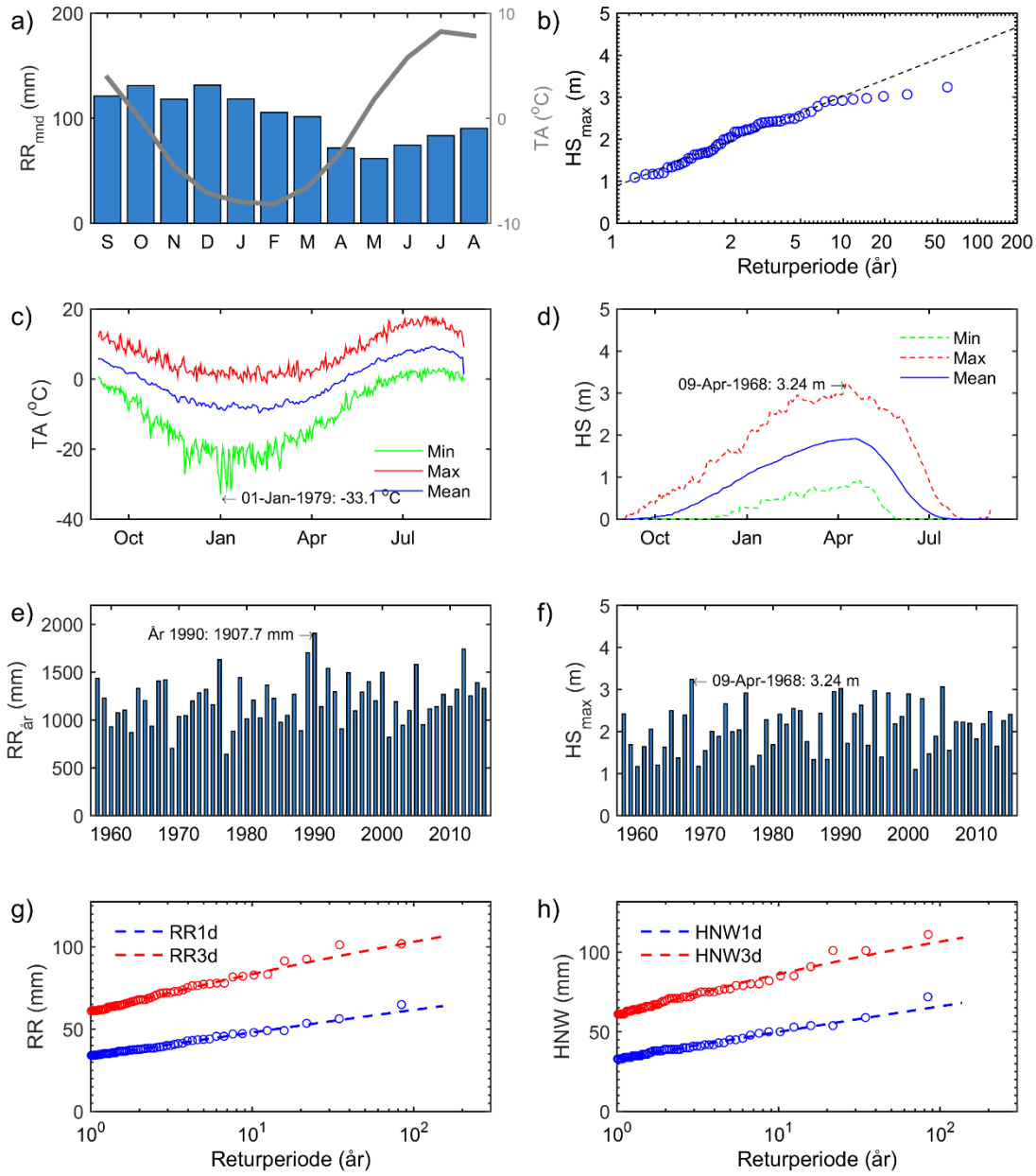

Figure 29 Climate profile for Fonnbu research station at Strynefjellet based on SeNorge data. a) Monthly precipitation (RR) and temperature (TA). b) Annual maximum snow height (HS) vs. return period and fit to Gumbel distribution. c,d) Daily minimum, maximum, and mean temperatures and snow heights. e,f) Time series of annual precipitation and snow height. g,h) 1- and 3- day precipitation and snow accumulation vs. return period (peak-over-threshold)

MATLAB library functions have been built to download time series of wind direction and wind speed for arbitrary locations from met.no's servers using OPeNDAP. It is possible to do this automatically for all days having precipitation as snow as defined by the

SeNorge data sets. Due to the large volumes of data involved when dealing with hourly resolution, and the fact that data is transferred from an external server, obtaining a time series for even a single location takes a relatively long time—a time series of 5 years can take 40 minutes to download. As a consequence, it has been decided that a closer evaluation of the usefulness of the data from this product should be conducted before further work based on it is planned.

6.3 Snow distribution using terrain indexes

An important project goal is to improve the tools used to analyze the spatial distribution of snow based on either wind observations from a selected location or a typical wind direction at snow precipitation events. The wind and precipitation data could either be observations or be based on gridded data. Snow distribution is highly dominated by terrain, and the simplest form of spatial snow distribution is therefore based on the dominant wind direction and the concomitant sheltering inferred from the terrain model.

The Winstral Sheltering Index for dominant wind directions has shown high correlation to observed snow distributions (Winstral et al., 2002). This was also tested at Finse, where the sheltering index, run for the main wind direction during the winter, was compared to the snow distribution at snow maximum, measured from a drone. The correlation is not perfect, but shows promising results (Figure 30).

The Sheltering Index for 8 different wind directions has been computed for all of Norway, applying the 10 m terrain model from the Norwegian Mapping Agency. The data is stored in netCDF files, with one file for each tile in the 10 m DEM containing sheltering indexes for 8 directions (see Figure 31 for an example of sheltered areas at westerly winds at Strynefjellet). These data sets are planned to be further used in a tool together with wind data. MATLAB-code has also been produced to compute the sheltering index for any terrain model.

K. Gisnås (NGI) participated in the Finse International Snow Workshop in October 2017, holding talks on snow measurements and computation of observed snow distribution using the Winstral terrain index. It was decided to work towards publication of snow measurements performed in cooperation with UiO in early 2018. Further cooperation with UiO related to UiO's snow drift and distributed wind measurements at Finse is also of interest to both parties.

6.4 Wind field simulations with WindSim

Build-up of WindSim competence has been initiated with a 2-day course for three of NGI's employees. Software and licenses have been purchased and installed centrally on NGI's Citrix platform. The software is built for optimizing wind farms and is prepared for input of rather coarse terrain models. For our purposes, high-resolution terrain features are of interest, and a GIS-tool has been built to prepare input files (terrain model

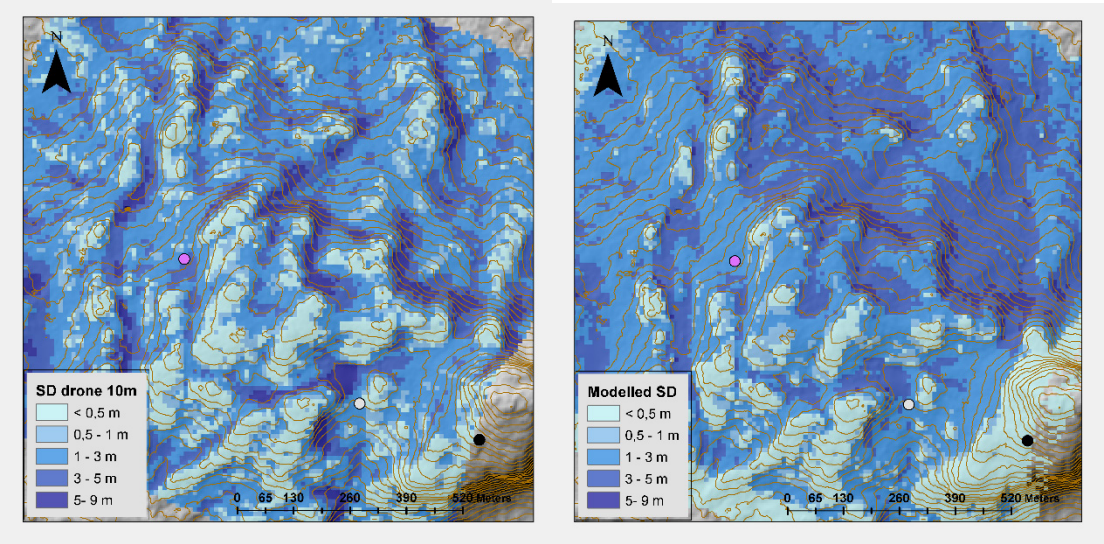

Figure 30 Observed (left) and modeled (Winstral; right) snow distributions over a 1.5 x 1.5 km² area at Vetle Hansbunuten, southeast of Finse

and terrain roughness) in the preferred format in WindSim. Here, the best available terrain model can be used, together with the CORINE 2006 land cover map.

One of the more interesting outputs from WindSim is a high-resolution wind field for a given wind direction, which allows for determining snow accumulation locations for storms with the same given dominant wind direction. This can been precomputed, e.g. for regions that are part of the avalanche warning service.

WindSim has been used to compute a snow distribution pattern for the Finse plateau, where snow distribution as mapped from drone observations is also available in high resolution (Figure 32 and Figure 33). This test was conducted using the default terrain models in WindSim (coarse resolution satellite-based terrain models). It was concluded that this is not sufficient to reproduce small-scale snow distribution, and further testing with higher-resolution terrain model inputs is necessary and planned for 2018.

An unforeseen amount of technical challenges related to software and installation has delayed the WindSim tests, and fewer tests than planned were conducted in 2017.

Figure 31 Winstral sheltering index for wind from west (270°) applied on the national 10 m DEM from the Norwegian Mapping Agency for Strynefjellet. Darker red colors indicate higher degree of sheltering and therefore areas more prone to snow accumulation

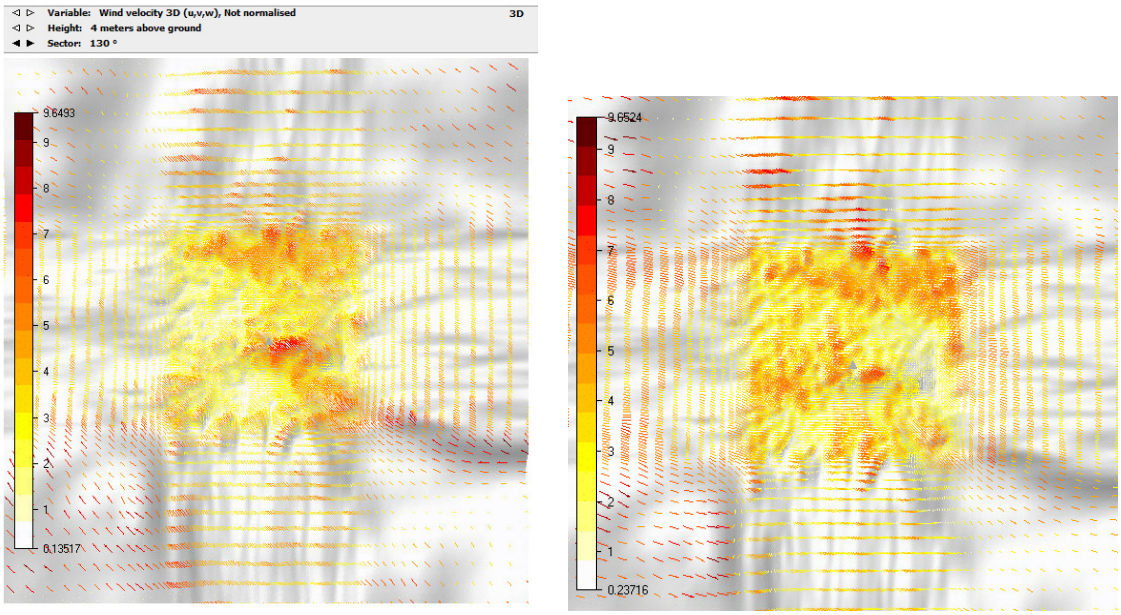

Figure 32 Examples of wind field simulations in WindSim, for wind directions of 130° (left) and 270° (right) at Finse

Results 2017

- SeNorge in-house dataset with extreme values for several return periods calculated for all of Norway
- KliNoGrid access
- WindSim license, built up in-house competence on wind simulations

Plans for 2018

- Further testing of KliNoGrid wind direction and combine with Winstral sheltering index
- Further development of snow probability using Senorge, KliNoGrid and Winstral.
- Further testing of WindSim and evaluation with wind observations and snow distribution data.
- Publication of snow distribution observations at Finse

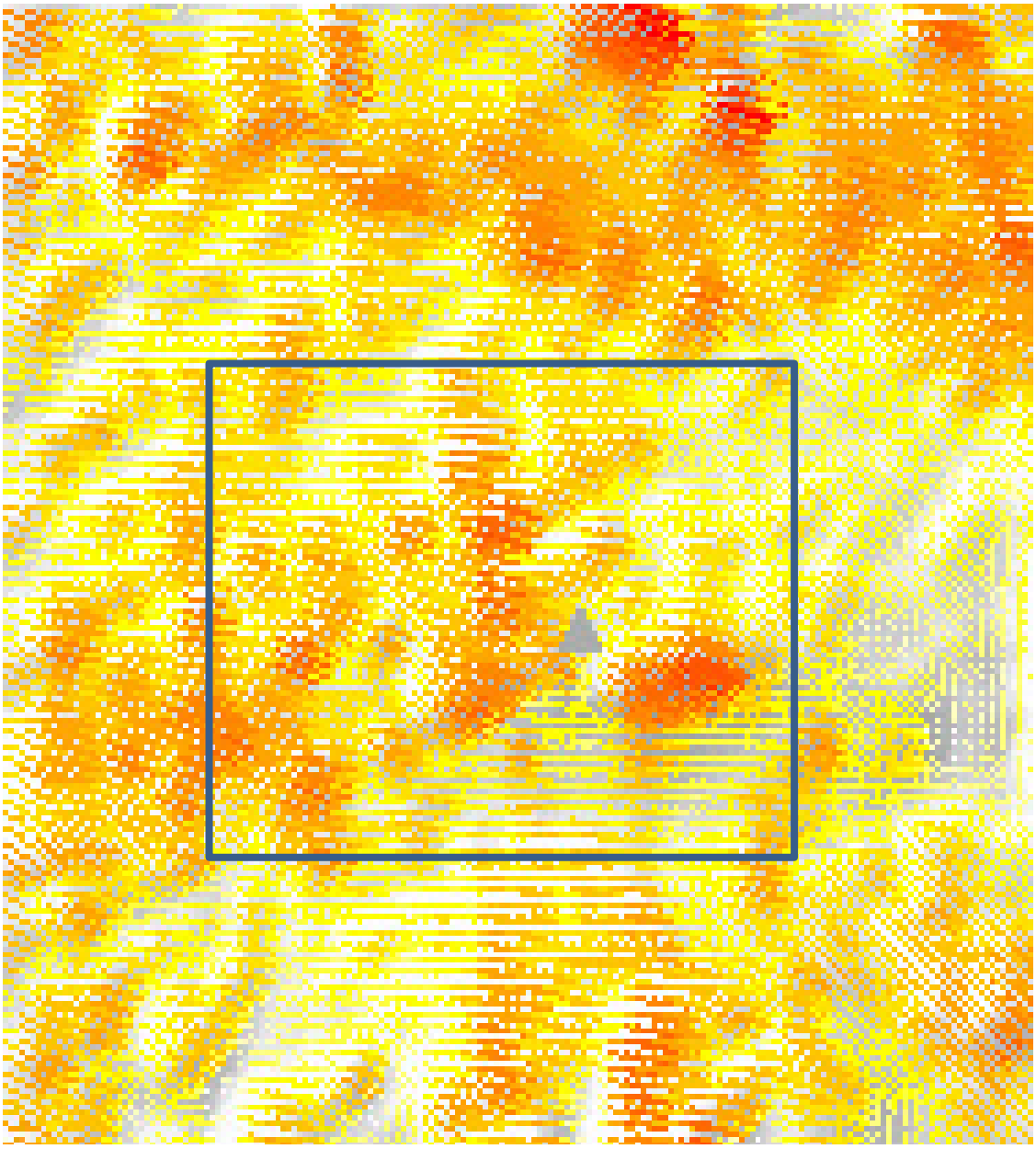

Figure 33 Wind field for winds from 270° at Finse shown in Figure 32 (right). Observed snow distribution shown in Figure 30 is indicated with blue rectangle. Colors are according to the legend in Figure 30

7 Work plan and budget 2018

7.1 The need for modifications to the work plan

The original work plan stipulated that work on StatPack, the new tool for taking into account statistical aspects in avalanche warning and hazard mapping (see Chapter 3 of this report) could be completed in 2017 with a moderate effort. In the course of the year, it became clear, however, that the necessary effort was significantly underestimated in 2016. Despite a budget increase of about 60% for this task in 2017, the important testing and fine tuning of the model to make it fully ready for practical use had to be deferred to 2018. Accordingly, funds need to be reallocated from other tasks in 2018 in order to achieve the goal.

7.2 Revised work plan 2018

The following changes relative to the original project description are necessary in 2018:

- Task T0.2 – Meeting of the advisory group will be carried out at the end of April in order to optimize its impact and to avoid the very busy period near the end of the year.
- The available funding for Task T1.5 – Model development is too low to produce extensive reports. Deliverable D1.2 is therefore integrated in the present report, and Deliverable D1.4 will be part of the Annual Report 2018.
- Task T2.1 – Development of StatPack is extended throughout 2018 to complete the work and to guide a MSc student from UiO in his work on testing the model. Deliverable D2.1 is accordingly rescheduled for completion by the end of 2018.
- To the extent possible, Task T2.2 – Effect of mitigation measures on land-use planning will be integrated into a collaborative project between Stryn municipality and NGI on the possibilities and necessary measures for allowing building in weakly endangered areas.
- Presumably Task 3.3 – Voellmy-type model for slushflows cannot be continued. Deliverable D3.1 can be produced only if sufficient funding can be allocated towards the end of the year.
- Task 3.2 – Methodology for slushflow forecasting will be reduced significantly because much of the necessary research work concerns indicators for slushflow danger at a regional level and thus NVE's avalanche forecasting activity. The reduced budget will be mainly used to follow up on, and support, ongoing research and development at NVE through seminars and discussions and to evaluate possible impacts of these developments for forecasting at the local level.
- As much as possible, Task T4.2 – Avalanche detection by infrasound will make use of the validation work for StatPack, which in turn makes extensive use of NGI's local forecasting for the National Road 15 at Strynefjellet and the frequent observations by the road maintenance crews.

- Due to the experienced delays and technical problems, Task 5.1 – Wind fields in the mountains will be continued in 2018 as long as required to achieve the goals. Task T5.2 – Estimation of snow transport rates under known wind conditions depends on our capability of reliably simulating wind fields in mountainous terrain and will therefore be deferred or—if necessary—canceled in this project period. Accordingly, Deliverable D5.1 is rescheduled for completion in 2018 and Deliverable D5.3 will be deferred or canceled.

7.3 Budget 2018

Table 5 Revised list of tasks and allocated budget for 2018

Task	Task description	Budget (kNOK)
T0.1	Administration, meetings	100
T0.2	Advisory group	150
T0.4	Reporting	100
	Total WP 0	**350**
T1.1	Running expenditures Fonnbu	150
T1.2	Maintenance Ryggfonn, Gudvangen	350
T1.3	Experiments Ryggfonn, Gudvangen	300
T1.4	Data analysis Ryggfonn, Gudvangen	200
T1.5	Model development	100
	Total WP 1	**1100**
T2.1	Testing and deployment of StatPack	450
T2.2	Impact of mitigation measures on land-use planning	100
	Total WP 2	**550**
T3.1	Snow cover simulation	100
T3.2	Methodology for slushflow forecasting	50
T3.4	Circum-Arctic Slushflow Network	50
	Total WP 3	**200**
T4.1	Avalanche observations	200
T4.2	Avalanche detection by infrasound	300
	Total WP 4	**500**
T5.1	Wind fields in the mountains	100
T5.3	Avalanche release probability	200
	Total WP 5	**300**
	Total FoU Snøskred 2017–2019 in 2018	**3000**

8 References

Bartelt, P., O. Buser, C. Vera Valero and Y. Bühler (2016). Configurational energy and the formation of mixed flowing/powder snow and ice avalanches. *Annals of Glaciology* **57**(71), 179–188

Beghin, P. and X. Olagne (1991). Experimental and theoretical study of the dynamics of powder snow avalanches. *Cold Regions Science and Technology* **19**(3), 317–326

Brattlien, K. (2017). Snøskredulykke ved Haugastøl 2017-03-15. NGI Technical Note 20170131-03-TN. Norwegian Geotechnical Institute, Oslo, Norway, 16 pages (in Norwegian)

Buser, O. and P. Bartelt (2015). An energy-based method to calculate streamwise density variations in snow avalanches. *Journal of Glaciology* **61**(227), 563–575

Domaas, U. and K. Gisnås (2017). Avalanches in the context of climate change in the northern regions. *Wildbach und Lawinenverbau* **81**(179), 70–79

Gauer, P. (2012). On avalanche (front) velocity measurements at the Ryggfonn avalanche test site and comparison with observations from other locations. In *Proceedings of the International Snow Science Workshop 2012*, Anchorage, Alaska, pages 427–432

Gauer, P. (2013) Comparison of avalanche front velocity measurements: supplementary energy considerations. *Cold Regions Science and Technology* **96**, 17–22

Gauer, P. (2014) Comparison of avalanche front velocity measurements and implications for avalanche models. *Cold Regions Science and Technology* **97**, 132–150

Gauer, P. (2017). Risikomangement in lawinenexponierten Gebieten Norwegens. *Wildbach und Lawinenverbau* **81**(179), 100–111 (in German with English abstract)

Gauer, P. (submitted). Considerations on scaling behavior in avalanche flow along cycloidal and parabolic tracks. *Cold Regions Science and Technology*

Gauer, P., D. Issler, K. Lied, and F. Sandersen (2008). On snow avalanche flow regimes: Inferences from observations and measurements. *Proceedings of the International Snow Science Workshop 2008, Whistler, British Columbia,* pages 717–723

Gubler, H. (1989). Comparison of three models of avalanche dynamics. *Annals of Glaciology* **13**, 82–89

Issler, D. (1998). Modelling of snow entrainment and deposition in powder snow avalanches. *Annals of Glaciology* **26**, 253–258

Issler, D. (2016). Incorporation of forest effects in MoT-Voellmy. NGI Technical Note 20160457-02-TN. Norwegian Geotechnical Institute, Oslo, Norway, 16 pages

Issler, D. (2017a). Notes on fluidization of snow avalanches by air expulsion from the snow cover. NGI Technical Note 20140053-03-TN. Norwegian Geotechnical Institute, Oslo, Norway, 18 pages

Issler, D. (2017b). Snøskyskredmodell SL-1D – Grunnleggende ligninger og korrekturfaktorer. NGI Technical Note 20170131-06-TN. Norwegian Geotechnical Institute, Oslo, Norway, 10 pages (in Norwegian)

Issler, D. (2018). Field Survey of the 2017-01-18 Rigopiano avalanche. NGI Technical Note 20170131-02-TN. Norwegian Geotechnical Institute, Oslo, Norway (in preparation)

Issler, D. and P. Gauer (2008). Exploring the significance of the fluidised flow regime for avalanche hazard mapping. *Annals of Glaciology* **49**(1), 193–198

Issler, D., P. Gauer, M. Schaer and S. Keller (1996). Staublawinenereignisse im Winter 1995: Seewis (GR), Adelboden (BE) und Col du Pillon (VD). SLF Interner Bericht 694. Swiss Federal Institute for Snow and Avalanche Research (SLF), Davos, Switzerland (in German).

Issler, D., J. T. Jenkins and J. N. McElwaine (2017). Comments on avalanche flow models based on the concept of random kinetic energy. *Journal of Glaciology*, DOI 10.1017/jog.2017.62

Issler, D., Á. Jónsson, P. Gauer and U. Domaas (2016). Vulnerability of houses and persons under avalanche impact – the avalanche at Longyearbyen on 2015-12-19. In *Proceedings of the International Snow Science Workshop 2016*, Breckenridge, Colorado, pages 371–378

Jónsson, Á. and C. Jaedicke (2017). Avalanches in the context of climate change in the northern regions. *Wildbach und Lawinenverbau* **81**(179), 182–187

Jordet, S., 2017. Validering av Snowpack for norske forhold – Mot en våtsnø- og sørpeskredindeks i Norge? MSc thesis, Department of Geosciences, University of Oslo. Oslo, Norway (in Norwegian). http://urn.nb.no/URN:NBN:no-60598

Lied, K., Bakkehøi, S., 1980. Empirical calculations of snow-avalanche run-out distance based on topographic parameters. *Journal of Glaciology* **26** (94), 165–177

McClung, D. M. and P. Gauer (submitted). Maximum frontal speeds, alpha angles and deposit volumes of flowing snow avalanches. *Cold Regions Science and Technology*

Humstad. T., Ø. Søderblom, G. Ulivieri, S. Langeland and H. Dahle, H. (2016). Infrasound detection of avalanches in Grasdalen and Indreeidsdalen, Norway. In *Proceedings of the International Snow Science Workshop 2016*, Breckenridge, Colorado

Kristensen, K. (2016). Assigning probabilities in local avalanche forecasting. In *Proceedings of the ternational Snow Science Workshop 2016*, Breckenridge, Colorado

Lunde, S., 2017. Infralyddeteksjon av snøskred og vurdering av konsept for automatisk integrasjon med database for snøobservasjoner. Norges teknisk-naturvitenskapelige universitet

Rapin, F. (1995). French theory for the snow avalanches with aerosol. *In:* G. Brugnot (ed.), *Actes de l'Université Européenne d'Eté – Neige et Avalanches, 14–25 septembre 1992, Chamonix, France.* Grenoble, Editions CEMAGREF, pages 163–172

Rauter, M., J.-T. Fischer, W. Fellin and A. Kofler (2016). Snow avalanche friction relation based on extended kinetic theory. *Natural Hazards and Earth System Sciences* **16**(11), 2325–2345

Salm, B. and H. Gubler (1985). Measurement and analysis of the motion of dense flow avalanches. *Annals of Glaciology* **6**, 26–34

Sampl, P. and M. Granig (2009). Avalanche simulation with SAMOS-AT. In *Proceedings of the International Snow Science Workshop 2009*, Davos, Switzerland, pages 519–523

Schaer, M. and D. Issler (2001). Particle densities, velocities and size distributions in large avalanches from impact-sensor measurements. *Annals of Glaciology* **38**, 321–327

Schaerer, P.A., and A. A. Salway (1980). Seismic and impact–pressure monitoring of flowing avalanches. *Journal of Glaciology* **26**(94), 179–187

Schweizer, J. and A. van Herwijnen (2013). Can near real-time avalanche occurrence data improve avalanche forecasting? In *Proceedings of the International Snow Science Workshop 2013*, Grenoble – Chamonix Mont Blanc, France, pages 195–198

Shimizu, H., T. Huzioka, E. Akitaya, H. Narita, M. Nakagawa and K. Kawada (1980). A study on high-speed avalanches in the Kurobe Canyon, Japan. *Journal of Glaciology* **26**(94), 141–151

Ulivieri, G., E. Marchetti, M. Ripepe, I. Chiambretti and V. Segor (2012). Infrasonic monitoring of snow avalanches in the Alps. In *Proceedings of the International Snow Science Workshop 2012*, Anchorage, Alaska, pages 723–728

Winstral, A., K. Elder and R. E. Davis (2002). Spatial snow modeling of wind-redistributed snow using terrain-based parameters. *Journal of Hydrometeorology* **3**, 524–538

Kontroll- og referanseside/ Review and reference page

Dokumentinformasjon/*Document information*		
Dokumenttittel/*Document title* Annual Report 2017		**Dokumentnr./*Document no.*** 20170131-05-R
Dokumenttype/*Type of document* Rapport / Report	**Oppdragsgiver/*Client*** Norges vassdrags- og energidirektorat (NVE)	**Dato/*Date*** 2018-01-12
Rettigheter til dokumentet iht kontrakt/ *Proprietary rights to the document according to contract* Oppdragsgiver / Client		**Rev.nr.&dato/*Rev.no.&date*** 0 /
Distribusjon/*Distribution* ÅPEN: Skal tilgjengeliggjøres i åpent arkiv (BRAGE) / OPEN: To be published in open archives (BRAGE)		
Emneord/*Keywords* Snow avalanches, full-scale experiments, field observations, dynamical and statistical models, slushflows, snowdrift		

Stedfesting/*Geographical information*	
Land, fylke/*Country* Norway, Italy	**Havområde/*Offshore area***
Kommune/*Municipality* —	**Feltnavn/*Field name***
Sted/*Location* —	**Sted/*Location***
Kartblad/*Map* —	**Felt, blokknr./*Field, Block No.***
UTM-koordinater/*UTM-coordinates* **Zone:** — **East:** — **North:** —	**Koordinater/*Coordinates*** **Projection, datum: East: North:**

Dokumentkontroll/*Document control*

Kvalitetssikring i henhold til/*Quality assurance according to NS-EN ISO9001*

Rev/ *Rev.*	**Revisjonsgrunnlag/*Reason for revision***	**Egenkontroll av/ *Self review by:***	**Sidemanns-kontroll av/ *Colleague review by:***	**Uavhengig kontroll av/ *Independent review by*:**	**Tverrfaglig kontroll av/ *Interdisciplinary review by:***
0	Original document	2018-01-08 Dieter Issler	2018-01-08 Ulrik Domaas		

Dokument godkjent for utsendelse/ *Document approved for release*	**Dato/*Date***	**Prosjektleder/*Project Manager***
	12 January 2018	Dieter Issler

NGI (Norwegian Geotechnical Institute) is a leading international centre for research and consulting within the geosciences. NGI develops optimum solutions for society and offers expertise on the behaviour of soil, rock and snow and their interaction with the natural and built environment.

NGI works within the following sectors: Offshore energy – Building, Construction and Transportation – Natural Hazards – Environmental Engineering.

NGI is a private foundation with office and laboratories in Oslo, a branch office in Trondheim and daughter companies in Houston, Texas, USA and in Perth, Western Australia

www.ngi.no

NGI (Norges Geotekniske Institutt) er et internasjonalt ledende senter for forskning og rådgivning innen ingeniørrelaterte geofag. Vi tilbyr ekspertise om jord, berg og snø og deres påvirkning på miljøet, konstruksjoner og anlegg, og hvordan jord og berg kan benyttes som byggegrunn og byggemateriale.

Vi arbeider i følgende markeder: Offshore energi – Bygg, anlegg og samferdsel – Naturfare – Miljøteknologi.

NGI er en privat næringsdrivende stiftelse med kontor og laboratorier i Oslo, avdelingskontor i Trondheim og datterselskaper i Houston, Texas, USA og i Perth, Western Australia.

www.ngi.no

NGI
OSLO
TRONDHEIM
HOUSTON
PERTH

NORWEGIAN GEOTECHNICAL INSTITUTE
NGI.NO

Main office
PO Box 3930 Ullevaal St.
NO-0806 Oslo
Norway

Trondheim office
PO Box 5687 Torgarden
NO-7485 Trondheim
Norway

T (+47)22 02 30 00
F (+47)22 23 04 48
NGI@ngi.no

BIC NO. DNBANOKK
IBAN NO26 5096 0501 281
ORGANISATION NO.
958 254 318MVA

ISO 9001/14001
CERTIFIED BY BSI
FS 32989/EMS 612006